MODEL JUNCTION ANALYSIS OF THE FRICTION AND WEAR OF METALLIC SURFACES

by

GEORGE KYTE FLEMING
B.E. Nova Scotia Technical College

A THESIS SUBMITTED IN PARTIAL FULFILMENT OF
THE REQUIREMENTS FOR THE DEGREE OF
MASTER OF APPLIED SCIENCE

in the Department
of
Mechanical Engineering

We accept this thesis as conforming to the
Required standard

THE UNIVERSITY OF BRITISH COLUMBIA
AUGUST, 1960

In presenting this thesis in partial fulfilment of the requirements for an advanced degree at the University of British Columbia, I agree that the Library shall make it freely available for reference and study. I further agree that permission for extensive copying of this thesis for scholarly purposes may be granted by the Head of my Department or by his representatives. It is understood that copying or publication of this thesis for financial gain shall not be allowed without my written permission.

Department of Mechanical Engineering

The University of British Columbia,
Vancouver 8, Canada.

Date August, 1960.

ABSTRACT

The adhesion theory of friction is investigated using the model junction proposed by A. P. Green in 1954. The results of the model junction experiments are extended to study the wear mechanism. An attempt has been made to correlate the model junction results with similar results obtained by various experimentors using actual surfaces.

The friction results established that friction is independent of load which is in agreement with experiments done using actual surfaces. The model junction shows general agreement with the theoretical estimate of the friction and normal forces made by A. P. Green.

The wear results indicate general correlations between the model and actual surfaces with regard to particle shape and wear-load relationships.

In general, the results of the investigation indicate that actual surfaces should have small surface finish angles for minimum wear and that the double shear mode of junction failure provides an explanation for wear particle formation and the large values of the coefficient of friction found for outgassed metals sliding in vacuo.

TABLE OF CONTENTS

CHAPTER PAGE

LIST OF FIGURES

FIGURE PAGE

A C K N O W L E D G M E N T

The Author wishes to take this opportunity to acknowledge the valuable assistance given to him by the faculty and staff of the Department of Mechanical Engineering.

Special thanks is extended to Dr. C. A. Brockley, who suggested the problem, for the many constructive criticisms he offered throughout the investigation.

CHAPTER I

I. INTRODUCTION.

The friction and wear of solid bodies in dry sliding contact are subjects of considerable practical and theoretical interest. The majority of the experimental work concerning friction and wear has been conducted using actual surfaces and the detailed study of complex interfacial phenomena under microscopic conditions is exceedingly difficult. The large scale model junction proposed by Green [1], would have many advantages in the study of friction and wear of metallic surfaces if correlation can be established between the model and actual surfaces. It is the purpose of this thesis to establish correlation and then use the model junction to study friction and wear under large scale simulated conditions. The specific similarities to be established are:

1. Wear particle shape.
2. Wear versus load.
3. Coefficient of friction as a function of load.

Having established the above similarities between the model and actual surfaces, these and other relationships will be studied in greater detail. In addition, the effect of velocity on the simulated coefficient of friction and wear will be investigated.

II. HISTORY *

A brief history of the various theories of friction is necessary in order to develop the reasoning leading up to the use of the model junction.

Amontons published the results of his experimental investigation of the friction of unlubricated solids in 1699. He hypothesized that the friction force was due to the interlocking of surface asperities and was equal to the force required to lift the irregularities of one surface over those of the other. Amonton's experiments with unlubricated surfaces indicated that the friction force was independent of the apparent area of contact of the surfaces. These experiments were verified by many investigators, including Hire (1732), Euler (1750), and Coulomb (1785). Coulomb made the additional observation that friction appeared to be independent of the sliding velocity. Rennie (1829) suggested that a more general theory should take into account the bending and fracture of the surface irregularities or asperities.

Ewing (1892) developed the adhesion theory of friction which suggests that the surfaces adhere together by the reaction of molecular forces following molecular displacement. This theory received considerable attention by Tomlinson (1929) and Hardy (1936).

Beare and Bowden [5], suggested that the

* This history is based on similar histories found in references 2 and 3 in the Bibliography. All the names mentioned in this section, unless otherwise specified, are found there.

frictional resistance between unlubricated metals could be attributed to the shearing of minute metallic junctions. These junctions could be formed by cold welding or adhesion when two asperities come into contact under extreme local pressure. Alternatively the welding could take place by the action of high local temperature, developed when the sliding velocity is large. This idea of junction formation is further established by Bowden and Leben in their observations of discontinuous sliding between unlubricated surfaces. They observed that the friction force would increase fairly rapidly and then suddenly diminish. This "stick-slip" behaviour is equivalent to the relaxation oscillations encountered in certain electrical circuits. Bowden and Tabor [4] have further shown that the area of contact may fluctuate in a similar manner. The adhesion theory of friction appears to be in agreement with the experimental data that has been accumulated. Additional contributions to the friction force have been suggested by Ernst and Merchant [7] and by Bowden and Tabor [2]. The former experimentors suggest that the friction force is increased on very rough surfaces by the force required to lift one surface irregularity over the other. It is of interest to note that this recent theory is equivalent to the original ideas of Amontons.

The latter group has shown the importance of a ploughing force, whereby the surface irregularities of

the harder surface plough out the softer one. These two additional contributions to friction are combined with the shearing component, resulting in the following equation,[3]

$$F = S + R + P_t$$

Where S is the shearing component of the friction force, R is the component resulting from lifting one surface irregularity over the other,

and P_t is the ploughing component determined experimentally by Bowden and Tabor.[2]

Feng [6] in 1952 proposed a new conception of the formation of metallic junctions. He suggested that the tips of two opposing asperities are roughened by plastic deformation, as a consequence they mechanically interlock as shown in Figure 1. Subsequently when one surface slides over the other, the junction shears some distance away from the interlocked interface. (Figure 1b). Feng suggests that the shear of the junction produces a temperature flash which causes heat to be conducted through the interface. If the temperature rise and heat conduction is sufficient to cause welding at the interface, metal will have been transferred from one surface to the other. In subsequent encounters with other asperities this transferred metal is likely to become detached as a wear particle.

In summary, it may be stated that various theories of friction have been advanced but the Bowden conception of metallic adhesion is the generally accepted theory at the present time. It is this theory which is utilized in the present work and it will be discussed in expanded detail in the next chapter.

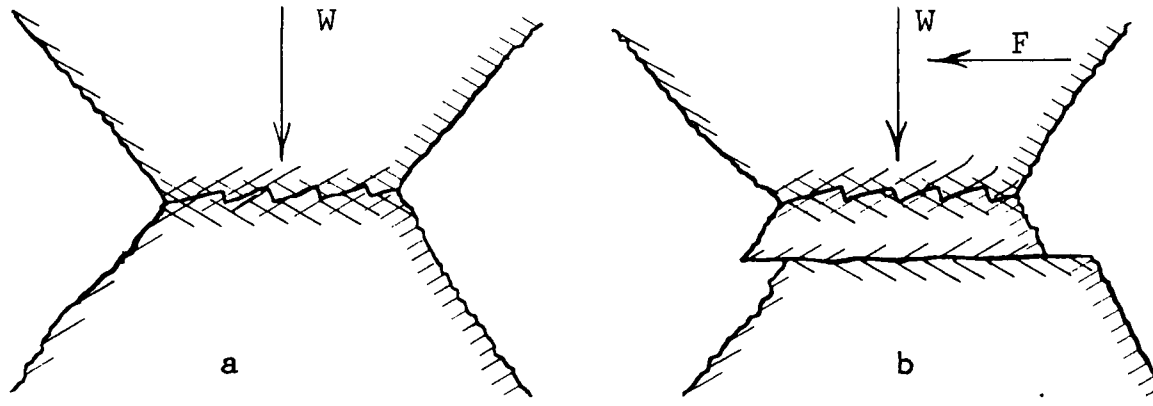

FIGURE 1

FENG THEORY OF METALLIC JUNCTION
FORMATION AND FAILURE

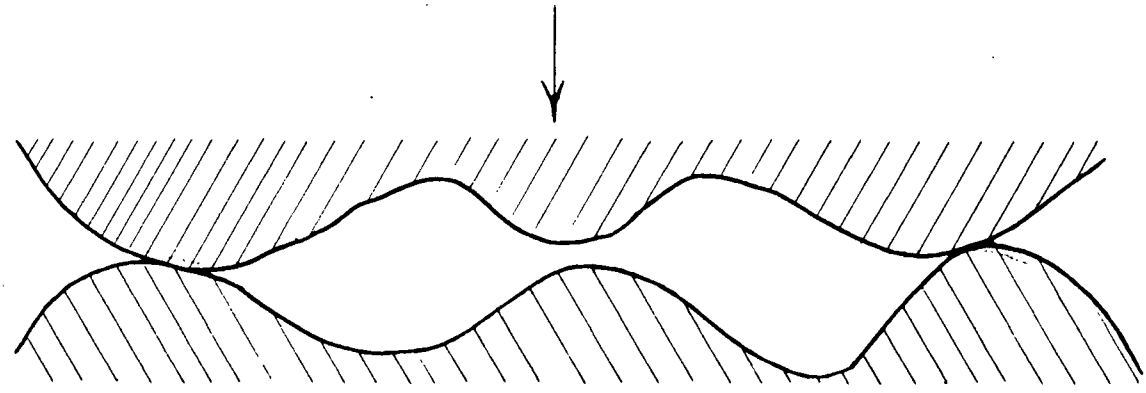

FIGURE 2

FORMATION OF METALLIC JUNCTIONS
BY ADHESION OR WELDING

CHAPTER II.

I. The Adhesion Theory of Friction.

Bowden and his co-workers have shown that when two surfaces are pressed together under a load, W, contact takes place at isolated asperities as shown by Figure 2. The local pressures at the points of contact exceed the plastic flow pressure p, of the softer material, and the asperities flow until the area A is sufficient to support the load without further deformation. That is

$$A = \frac{W}{p} \quad \text{------(1)}$$

The plastic flow at the interface of two asperities can produce the cold welding and junction formation previously discussed. These junctions must be destroyed in order for sliding to take place. The force F required to shear the junction is

$$F = sA \quad \text{- - - - - - (2)}$$

where s is the bulk shear stress of the softer material. By combining (1) and (2) we arrive at the following expression for f, the coefficient of friction;

$$f = \frac{F}{W} = \frac{s}{p}$$

and we note that the friction force is dependent only on the bulk strength properties of the material. However, s and p are interdependent, and are related by Von Mises's criterion for plastic yielding, namely:

$$p^2 + 3s^2 = Y^2$$

where Y is the yield stress of the material. consequently no absolute solution can be obtained and

a calculated value of f is indeterminate.

II. The Model Junction

In 1955 Green[8] adopted a different approach whereby he suggested that the junction accepts load in a manner determined by the deformation process. He assumed that the deformation of a single asperity pair took place in a particular manner. From plasticity theory, using plane strain conditions, i.e. the strain is assumed zero in the width direction, Green determined what contribution the junction made to the load and friction during its "life cycle."

The following assumptions were made in this theoretical analysis.

1) The sliding between the surfaces was so slow that temperature effects were negligible.

2) Steady sliding was assumed to prevail and this implied parallel sliding as demonstrated by Figure 3. At 'a' a metallic junction is being formed between to asperities which have a relative motion in the direction of the arrows. The junction can still grow due to the relative motion of the asperities and this action takes place during the sliding process. Steady sliding is demonstrated in Figure 3b, where the junction has ceased growing and the relative motion of one surface with respect to the other is parallel.

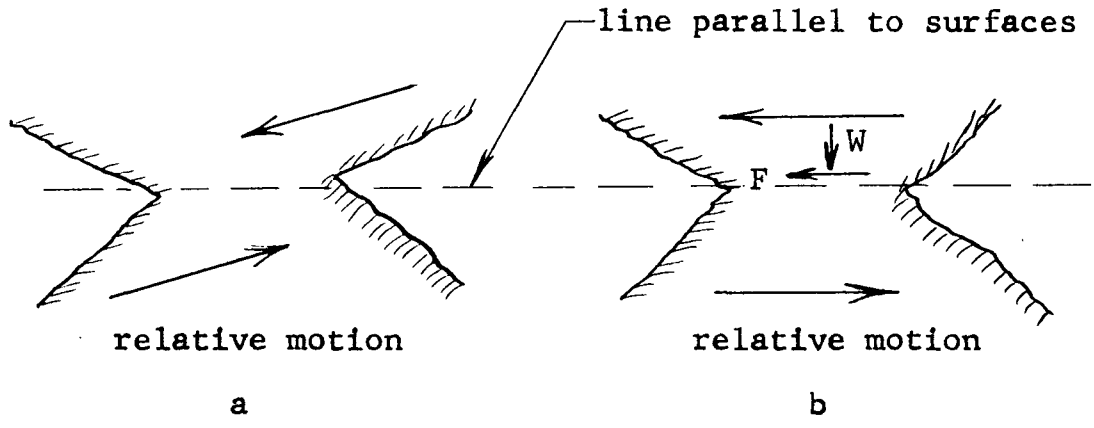

FIGURE 3

DIAGRAM OF A JUNCTION
(a) DURING THE INITIATION OF SLIDING,
(b) DURING STEADY SLIDING

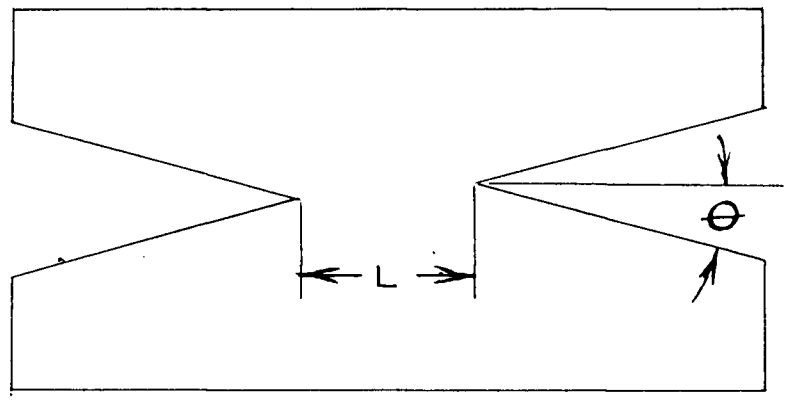

FIGURE 4

GREEN'S MODEL JUNCTION

Using the above assumptions and the Bowden theory of metallic junction formation Green derived a model junction, the parameters of which he used in his theoretical analysis. Green's model was of the shape shown in Figure 4. θ is the angle of surface finish of the surfaces and L is the width of the junction and is dependent on the previously defined strength properties of the material, i.e. the bulk shear stress s and the plastic flow pressure p. The results of the plasticity study are shown graphically in Figure 5, both for a junction in which there is a strong welding at the interface, and a weak junction where the adhesion is insufficient to prevent relative sliding at the interface. It is to be noted that the strong junction has a fairly constant friction force and the load supporting force reaches a maximum value early in the cycle.

On the other hand the friction force of the weaker junction reaches a maximum early and diminishes, a result which can be attributed to the interfacial sliding previously mentioned. From a ratio of the areas under the F and W curves, he arrived at a coefficient of friction for the strong junction of approximately 1. For the weak junction a very small coefficient of friction of 0.2 was obtained. The former is of the order of magnitude of the value found for "clean" metals sliding in air. The latter value is much lower, not only due to interfacial sliding but also due to the fact that weak adhesion reduces the shear strength of the junction.

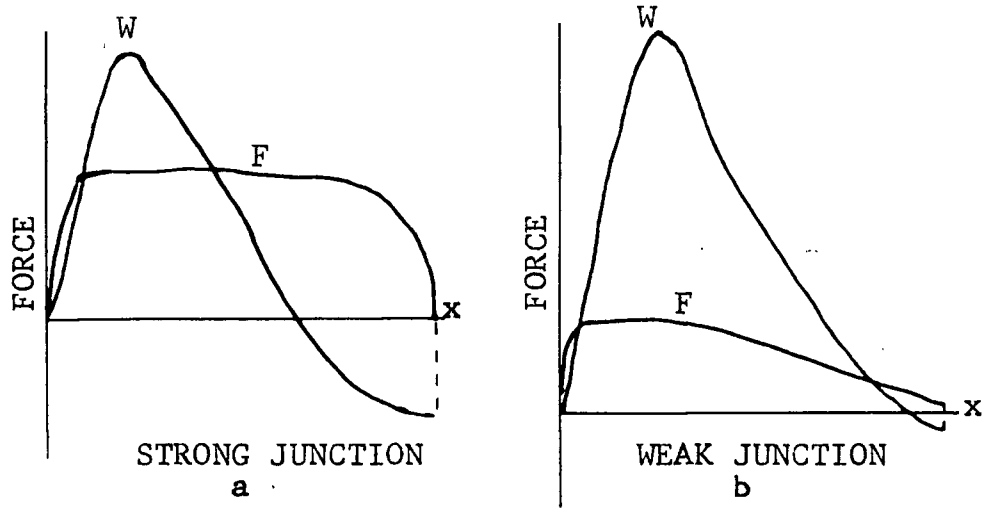

FIGURE 5

GREEN'S THEORETICAL ESTIMATE
OF THE FORCES INVOLVED IN
THE FRACTURE OF A METALLIC JUNCTION

Greenwood and Tabor investigated Green's model junction theory further by making junctions out of a single piece of sheet metal to simulate perfect adhesion of the strong junctions. These simulated models were then broken in an apparatus in which one asperity was held fixed and the other moved parallel to it according to the condition of steady sliding.

The machine was fitted with cantilever beams, the deflection of which gave the normal load and friction force. For the three types of junctions tested, namely, soft copper, hard copper and aluminum with surface finish angle θ approximately equal to 10^{o}, the coefficient of friction in all cases was found to be near 3. This is considerably larger than the normally observed value for unlubricated metals sliding in air. However, the value is of the same order as that obtained for chemically clean surfaces sliding in vacuum. The difference is explained by the fact that actual surfaces nearly always are coated with oxide or other contaminent film and strong adhesion is impossible.

III. Wear

It is logical to extend the model junction simulation to a study of wear mechanism. Before discussing the metallic junction and wear, it is convenient to review the basic wear processes. The three major types of wear mechanisms are illustrated diagramatically by Figure 6.

THREE BASIC TYPES
OF WEAR

I CORROSION

II PLOUGHING AND FATIGUE

III ADHESION

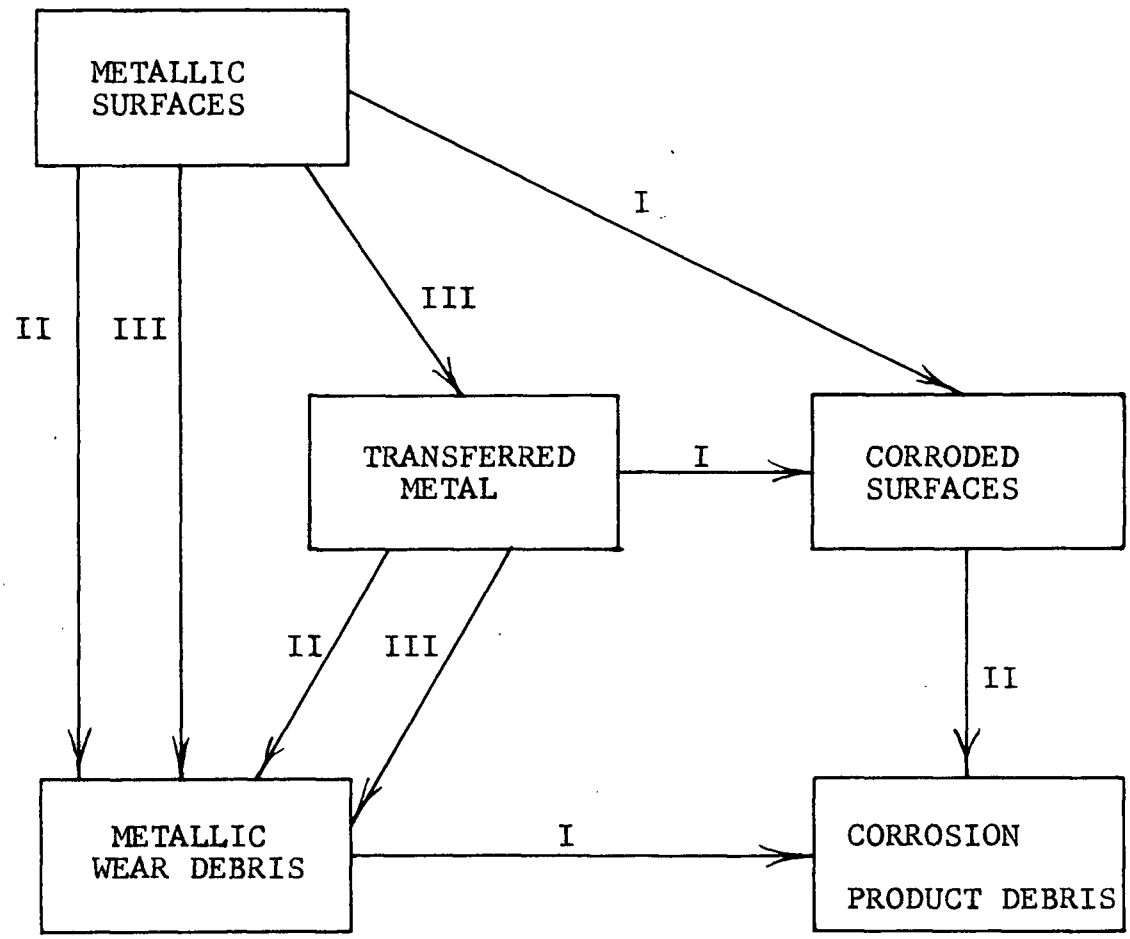

FIGURE 6

WEAR MECHANISMS

Since in most all practical systems wear occurs in combinations of the basic processes, it is of interest to examine their inter-relationships. Corrosive wear can result from contaminents on any surface, path I - II or a surface resulting from metal transfer path III - I - II. The corrosion debris on the contaminated surfaces is produced by a ploughing or fatigue of the contaminent film. Corrosion of actual metallic wear particles is also possible in the presence of a contaminating agent, paths II - I and III - I.

The ploughing type of wear mechanism predominates at the time bearing surfaces are "running in", when they are relatively rough. This process can produce wear debris directly (II), or from a surface that is the result of metal transfer path III - II. The fatigue process results from repeated stressing of the bearing surfaces, resulting in direct wear debris.

The third process, adhesion, has been referred to above in describing the other two wear mechanisms as metal transfer. This mechanism is the direct result of the fracture of Bowden's metallic junction. The shearing of these junctions can take place in three different ways, depending on the surfaces.

1) If the junction is weaker than the metals of which it is formed, it will fracture at the interface and very little, if any, wear debris will result.

2) A junction formed at the interface of asperities of dissimilar metal will fracture in the bulk of the softer material. This will result in a particle adhering to one surface which could be dislodged in a subsequent encounter with another asperity. If the metallic transfer progresses to a conclusion, similar surfaces will result. These two surfaces will then wear as surfaces of similar metals, path III.

3) Junctions formed between surfaces of similar metal will fracture at some distance from the weld and since the asperities have the same strength properties they should both fracture equally. This will result in the direct formation of a wear particle, path III. This is the wear process involved in the fracture of the model junctions to be investigated in this work.

Green [8] observed the formation of such particles in his qualitative examination of the fracture of plasticine models. Greenwood and Tabor [10] observed a few isolated cases of a "knot" of metal forming during the deformation of some of their metallic model junctions. Brockley [11] examined the direct wear particle mechanism using the model junction and he found that small symmetrical lens-shaped particles could be formed. He concluded that the formation of the particle was dependent on the geometry of the junction, and he conducted further experiments in this direction [12].

The mode of failure studied by Brockley is not only a representative wear mechanism but the "double shearing", that is, the shearing of both sides of the

junction simultaneously, is thought to add considerably to the friction force.

It is contended in this investigation that if this mechanism can be duplicated in the revised apparatus, where the friction force and load carrying force can be measured, the higher values of the coefficient of friction encountered when clean metals slide in a vacuum might be approached.

To summarize, the simulated friction and wear mechanism will be analyzed, with particular attention being given to the effect of the double shear failure on the coefficient of friction.

CHAPTER III.

EXPERIMENTAL

The experimental work was carried out according to the assumptions utilized by Green in his theoretical analysis of the model junction. The assumptions are re-stated as follows:

1) Sliding between unlubricated similar metals at speeds so slow that any surface temperature effects are negligible. In the present investigation the velocity of sliding was of the order of one hundredth of an inch per minute.

2) Steady sliding between clean metals in vacuum which implies that the surfaces move parallel to one another. This condition was established in the design of the apparatus.

I. The Model Junction

A) Geometry - The geometry of metallic surfaces can be determined by taper section, electron microscope and surface analyzer techniques. The shape of metallic junctions, formed from these surfaces of known shape was derived basically from the manner in which the metallic junctions on actual surfaces are assumed to be formed. Referring to Figure 7, one surface "a" is moving parallel to a fixed surface "b", in the direction shown, with contact established between two asperities. This encounter is shown in Figure 7b, and it is assumed that the asperities form a junction by the adhesion process.

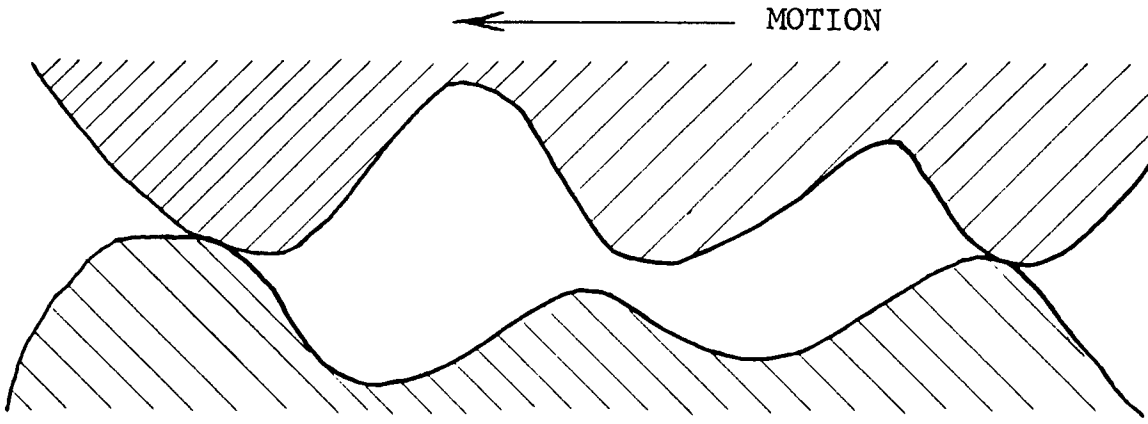

A

JUNCTION FORMATION

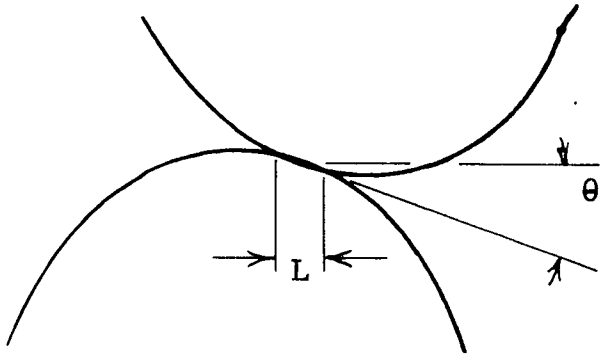

B

A METALLIC JUNCTION

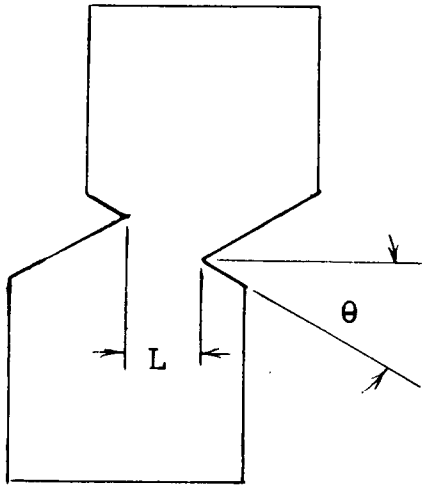

C

MODEL JUNCTION

FIGURE 7

DERIVATION OF THE MODEL JUNCTION

The shape of the junction can be defined by the parameter θ, the angle of the surface finish and L the horizontal projection of the area of contact, which is assumed to depend on the load. The model junction is derived from the actual deformation process and is shown in figure 7c. The parameters L and θ are defined in relation to the actual junction previously discussed. The models were made with straight sides and sharp corners.

On actual surfaces the angle θ varies from approximately 4^{o} to 30^{o}, [11, 12]. The dimension L which has been defined as the load factor was varied between ¼ inch and 7/8 of an inch. It is of interest to note that the size of the model is approximately one million times the size of actual junctions.

Actual junctions are three dimensional, of conical or pyramidal shape. However, in the present work two dimensional models were used, whereby the thickness was much smaller than the other two dimensions. In order to study the plane strain effect, which was also studied by Green (see page 8, Chapter 2) thicker models were used at one stage of the research.

B) Material - The junctions were fabricated from a single piece of 1/8" thick sheet copper to simulate perfect adhesion. Copper was used since it was a representative pure material with distinctive work hardening properties. The few thick junctions investigated to show the effect of plane strain were 5/16" thick. The copper was A.S.T.M. specification B152, Electrolytic Tough Pitch Copper, containing 99.92%

copper and a trace of iron. Several tensile specimens were taken from the sheet and broken in the Olsen testing machine. The average strength of the specimens in the "as received" condition was 33,800 psi and the hardness was 78.5 on the Rockwell E** scale. The annealed specimens had an average tensile strength of 30,700 psi and a hardness of 55.7 on the Rockwell H* scale. The exact reduction that the copper had undergone during manufacture was unknown but from a comparison between the tensile test results and published data,[15] it was found to be approximately 10%.

C) Metallurgical - The model junctions were annealed at 470°F for 2½ hours and quenched in water in order to maintain a homogeneous material throughout the experiments. After annealing all the junctions were checked for hardness to confirm the quality of the heat treatment.

II APPARATUS

A) Design Considerations

The apparatus was designed using as a basis the simple machine used by Brockley[10], shown in Figure 8. The model junction was mounted as shown. The moving block was guided by the rails C, the power being supplied through the screw and crank arrangement D. Essentially the same ideas are incorporated in the new apparatus.

** Rockwell E Scale - 1/8" Balland 100 Kilogram weight.

* Rockwell H Scale - 1/8" ball 60 Kilogram weight.

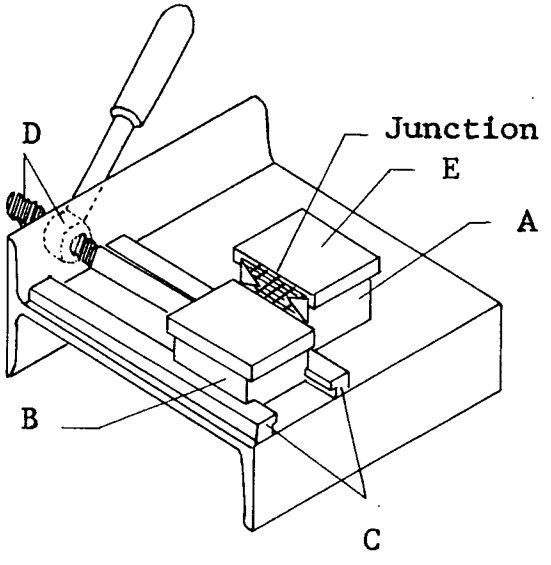

FIGURE 8

MODEL JUNCTION TESTING APPARATUS USED
BY BROCKLEY

The machine used by Greenwood and Tabor [8] was slightly more elaborate than the one described above. It provided for the measurement of the simulated friction and load forces, by utilizing a system of cantilever beams.

The basic differences between the above mentioned machines and the one used in the present work are: firstly, the new machine is more rigid, and secondly, it is power-driven.

The design of the new machine required that it be much more rigid than its predecessors. When the machine in Figure 9 was first used, the rails were bolted and pinned to the frame. It was found that a number of the early junctions broken produced a "particle" or a knot of metal; later on, when the machine lost its initial rigidity, due mainly to the deflection of the rails, particles were no longer obtained. However, when the rails were welded to the frame, the previous results were duplicated. The method of force measurement used by Greenwood and Tabor required large beam deflections, and it would appear that these deflections influenced the mode of junction failure. Accordingly in the present work a method of force measurement was devised which gave rigidity coupled with sensitivity. The method involved the use of a "strain ring" which will be described later.

The new apparatus is power-driven by a servo-controlled motor. This gave the advantage of control over the rate of travel of the moving asperity.

The final design consideration was the magnitude of the forces involved in breaking a particular junction. To determine this, one of the larger junctions used by Brockley[10] was mounted in the small apparatus, then the apparatus was set up in an Olsen testing machine and the simulated friction force was obtained over the life of the junction. The results of these tests are contained in Appendix A. Comparing these with Greenwood and Tabor results, some idea of the simulated load was obtained. With a knowledge of these forces the various components of the new apparatus were designed.

B. Description of Apparatus

The new machine is illustrated in Figure 9 with the various components noted.

The machine operates in the following manner: The motor (1) drives the power screw (2) through the two gear boxes (3) and a chain drive (4). One asperity of the model junction is attached by plates (5) to the moving block (6) which travels in the guides (7) parallel to the fixed block (8). The fixed block holds the strain ring (9) to which the other asperity is retained by plate (10).

The servo-motor gives a constant output torque over a range of speeds from 3600 rpm to 36 rpm. With the speed reduction and the power screw this gives a range of sliding velocities between 0.734 in/min and 0.00734 in/min.

As stated above, the main reason for using a

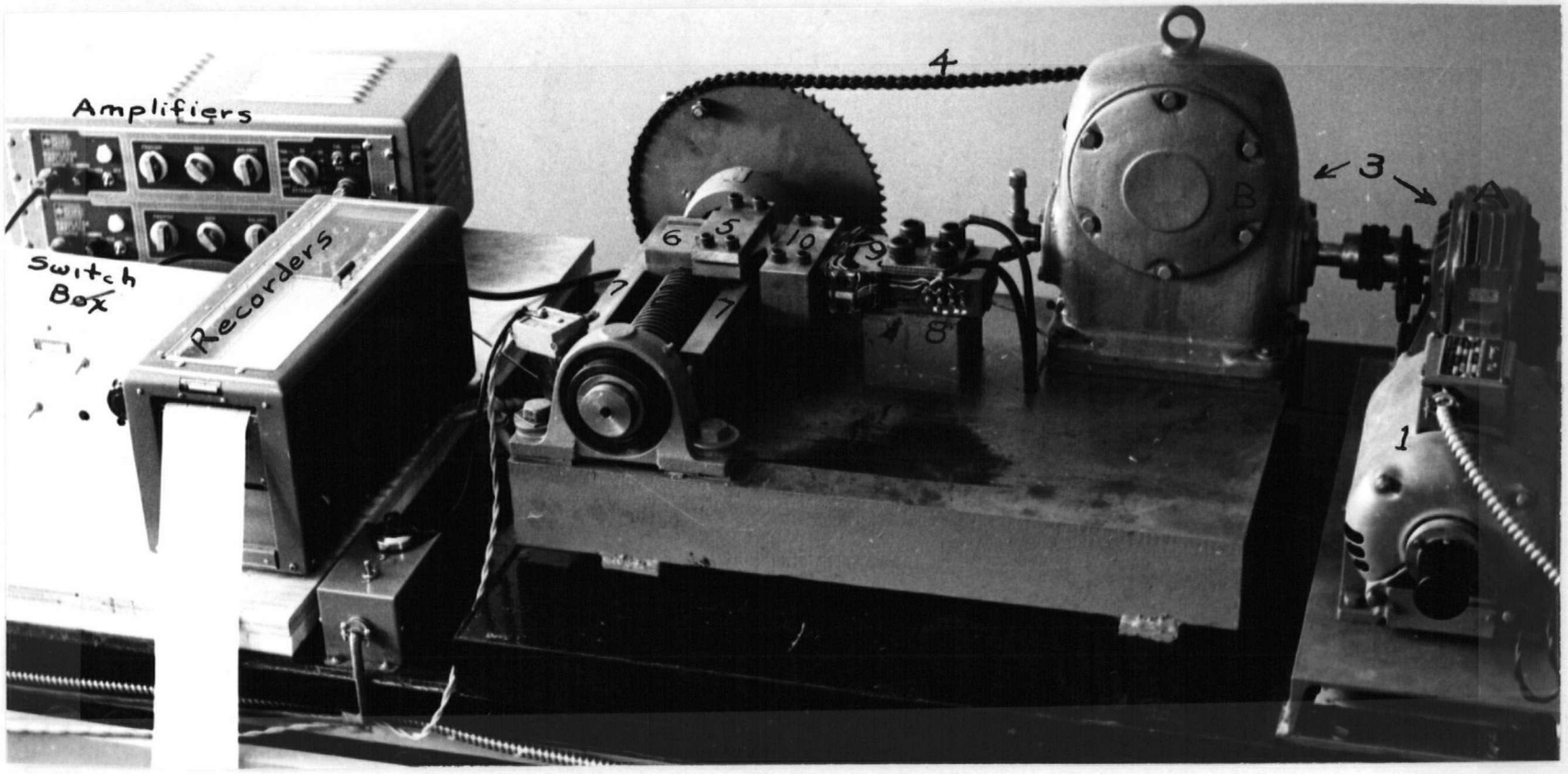

FIGURE 9

1. Servo-motor
2. Power screw
3. Gear Reducers A 40:1
   B 17.5:1
4. 70:30 Chain Drive
5. Holdown Plate
6. Moving Block
7. Guides
8. Fixed Block
9. Strain Ring
10. Holdown Plate

strain ring was to achieve rigidity of the apparatus. Similar strain rings are used in machine tool dynamometers and design information is available in the literature[16].

Eight strain gauges arranged as shown in Figure 10 measure the W and F forces when connected in the correct manner in a Wheatstone Bridge. The Bridge connections and the detailed drawings of the strain ring, as well as the design equations are given in Appendix B.

The signals from the strain ring are fed into a switch box, then into Edin amplifiers and a continuous recording of the simulated friction and load were obtained on a two-channel oscillograph.

The rate of travel of the moving block was calibrated against the oscillograph chart. This made it possible to obtain the total junction travel from the chart as well as correlating the two forces with the actual junction displacement.

The strain ring and allied equipment was calibrated in an Olsen testing machine according to the procedure described in Appendix B. The calibration curves for various amplifier attenuations are also found in Appendix B. During calibration cross-sensitivity effects were noted. The cross-sensitivity of the friction force on the equivalent load is taken into account since the friction force is generally three times the normal load (see Results). The effect of W on the friction force is only about 1.5 per cent of F and is therefore neglected; this can be readily verified by examining the calibration curves.

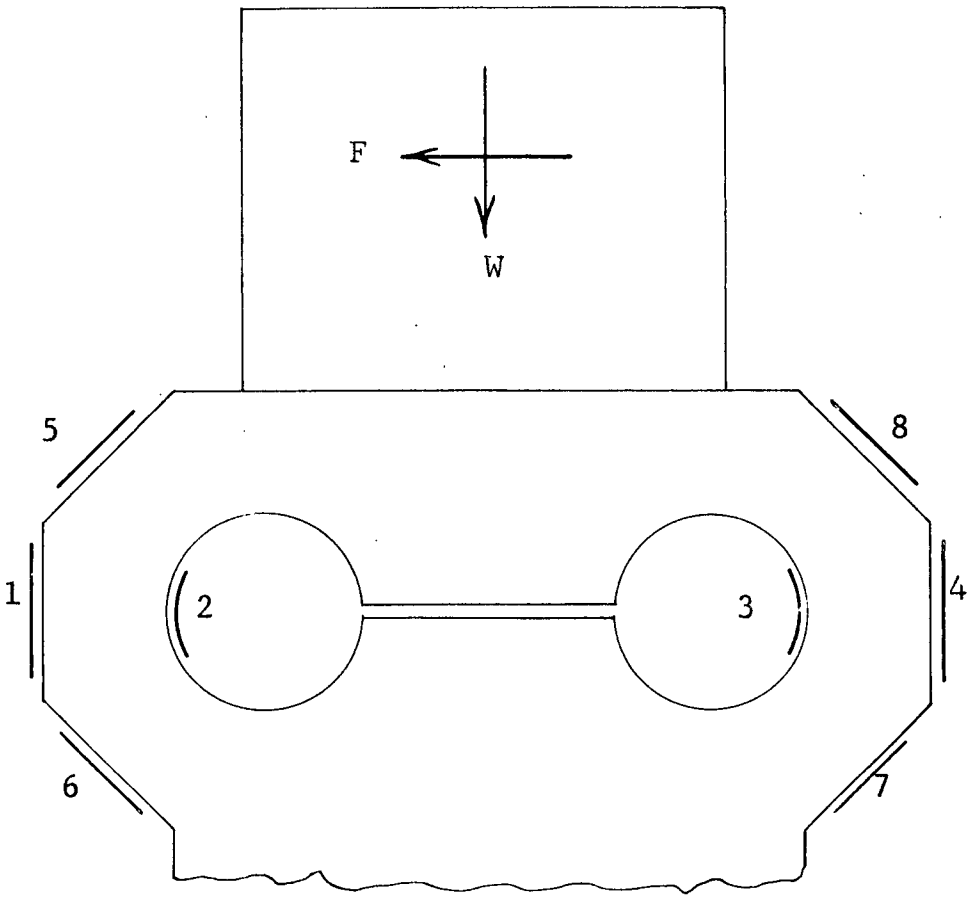

FIGURE 10

F - Bridge gages 1, 2, 3 and 4
W - Bridge gages 5, 6, 7 and 8

STRAIN RING - SHOWING
LOCATION OF GAGES

In summary, the present apparatus appears to be more rigid than earlier models. The provision of velocity control made it possible to study the effect of this important variable on friction and wear.

III Experimental

Experiments were performed in such a way that both a friction and a wear analysis could be carried out on the same junctions. The first models were stamped with a one-tenth inch grid so that the deformation process could be readily observed and photographed. All experiments were conducted at a sliding velocity of 0.202 in/min. with the exception of those in which the velocity was varied to determine its effect on friction and wear. A continuous trace of the simulated friction and load forces was obtained so that the coefficient of friction could be determined at any point as well as the average f over the "life" of the junction.

The simulated wear of the various junctions was assessed on the basis of the weight of the particles formed.

CHAPTER IV

RESULTS

The results of the investigation are divided into two main sections, wear and friction. The wear results are presented qualitatively and in graphical form while the friction results are all in graphical form. A photo-elastic model was examined and these results are included in the wear section.

I WEAR

A. Wear Particle Formation

The manner in which metallic junctions could deform and fracture, forming wear debris was studied using the model junction. Sequence photographs of the deformation of a typical model junction are given in Figure 11. The junction has a surface finish angle θ of 30^{o} and a load factor L of 0.65 inches. A 1/10 inch grid was stamped on the junction to show the deformation process. The first photograph shows the junction before deformation has taken place. The next picture illustrates the initiation of fracture and it is evident that the failure did not start at the notches but a short distance from them. Stress concentration at the notches, caused those areas to become work hardened by the initial deformation so that fracture took place in the softer metal some distance from the notches. In the third photograph a particle has started to take shape and a double shear mode of failure is evident. It was observed

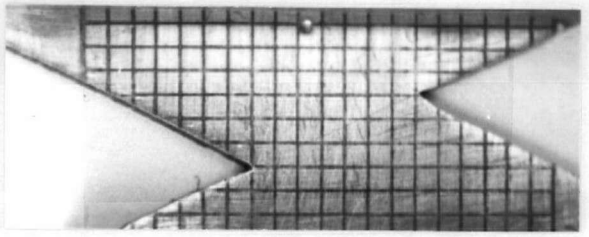

a

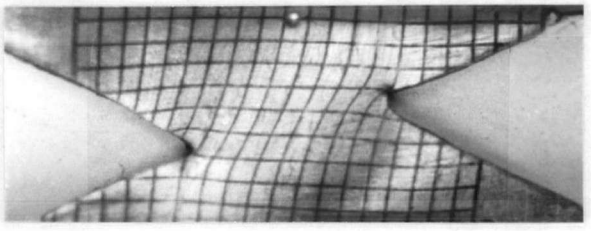

b

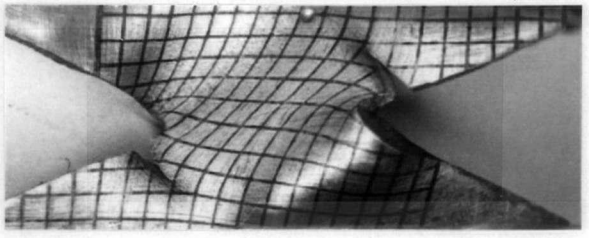

c

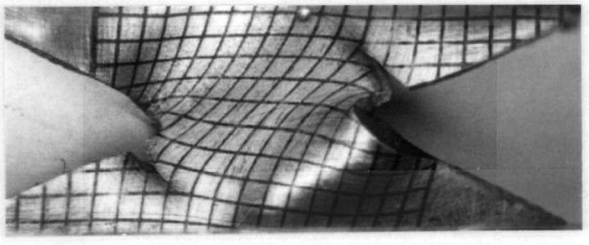

d

FIGURE 11

SEQUENCE PHOTOGRAPHS
OF THE DEFORMATION OF
A MODEL JUNCTION

θ = 30 degrees L = 0.650 inches

in this type of failure that the tearing did not take place simultaneously on both asperities, but would proceed on one side then stop and continue on the other. The picture also shows evidence of 'out of plane bending' that is bending in a plane perpendicular to the plance of the junction and perpendicular to the direction of motion of the moving asperity. At this stage Green's plane strain assumption ceases to be valid. However, it is to be noted that failure was initiated under near plane strain conditions as seen in the second photograph. The out of plane effect is pronounced in the last picture of the sequence, where the simulated wear particle has twisted perpendicular to the plane of the junction. Further deformation of the junction resulted in the particle adhering to one asperity, or the other. This indiscriminate adherence of the wear particle was found when several similar junctions were investigated.

B. Photo-elastic Investigation of A Model Junction

The method used was a photo-elastic coating technique which allowed the structure to be tested in the actual loading system. The method was ideal for a study of the stress distribution in a model junction. In this method a thin piece of a suitable bi-refringent polymer is attached to the metal structure with a reflective cement. When the photo-elastic coating is subjected to polorized light and viewed through an analyzer the lines of constant shear stress at the interface between the plastic and the structure can be seen.

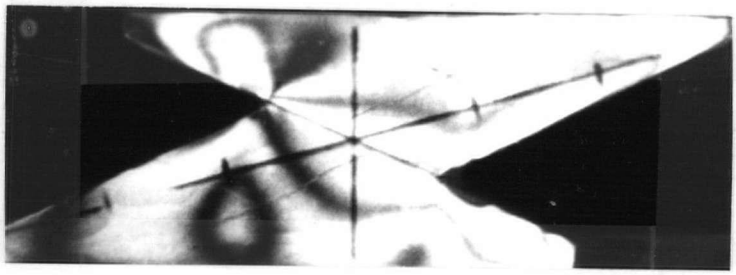

a

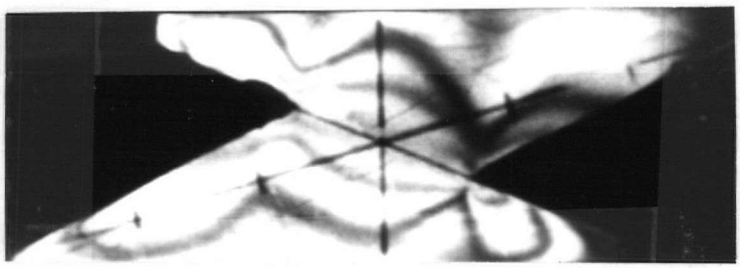

b

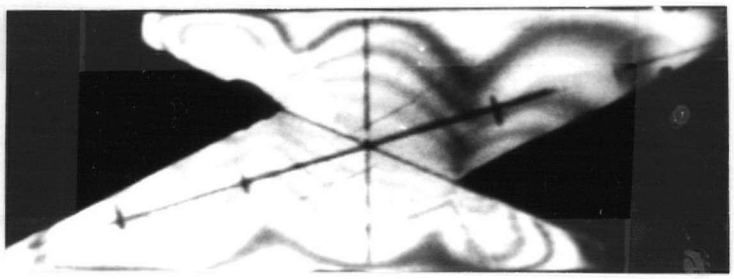

c

FIGURE 12

RESULTS OF PHOTOELASTIC
INVESTIGATION SHOWING
STRESS CONCENTRATION AND
MAXIMUM SHEAR STRESS LINES

In this investigation the plastic used was of the Photostress Zandman Method type, 0.119 $\pm$ 0.002 inches thick. The material was cut to the shape of the central portion of a junction with $\theta = 25^{o}$ and L = 0.625 inches. and cemented to an actual junction. The model was then placed in the apparatus and strained. The results obtained were only qualitative and are presented in figure 12. At 'a', under a very slight deformation, the stress concentration at the notches is quite evident. With more displacement, the constant shear stress fringes appear (figure 12b) and multiply with further stressing (figure 12c).

The complete quantitative results of the wear investigation follow.

C. Wear versus Surface Finish Angle

Figure 13 shows the variation of simulated wear with surface finish angle for various load factors. The surface finish angles and load factors were arrived at from the discussion given in Chapter III. There is some scatter of the points especially at the smaller load factors and angles. At a surface finish angle of 20 deg. there were no particles formed for load factors of 0.875 inches and 0.625 inches, although there are numerous other points both at greater and lesser angles. It is also evident that the particles formed with the 20 deg. junctions are displaced from their curves.

The general trend of the curves is towards zero wear at approximately 10 deg. The slopes of the lines are positive and vary from 0.0353 for L = 0.875 inches to 0.0154 at L = 0.54 inches.

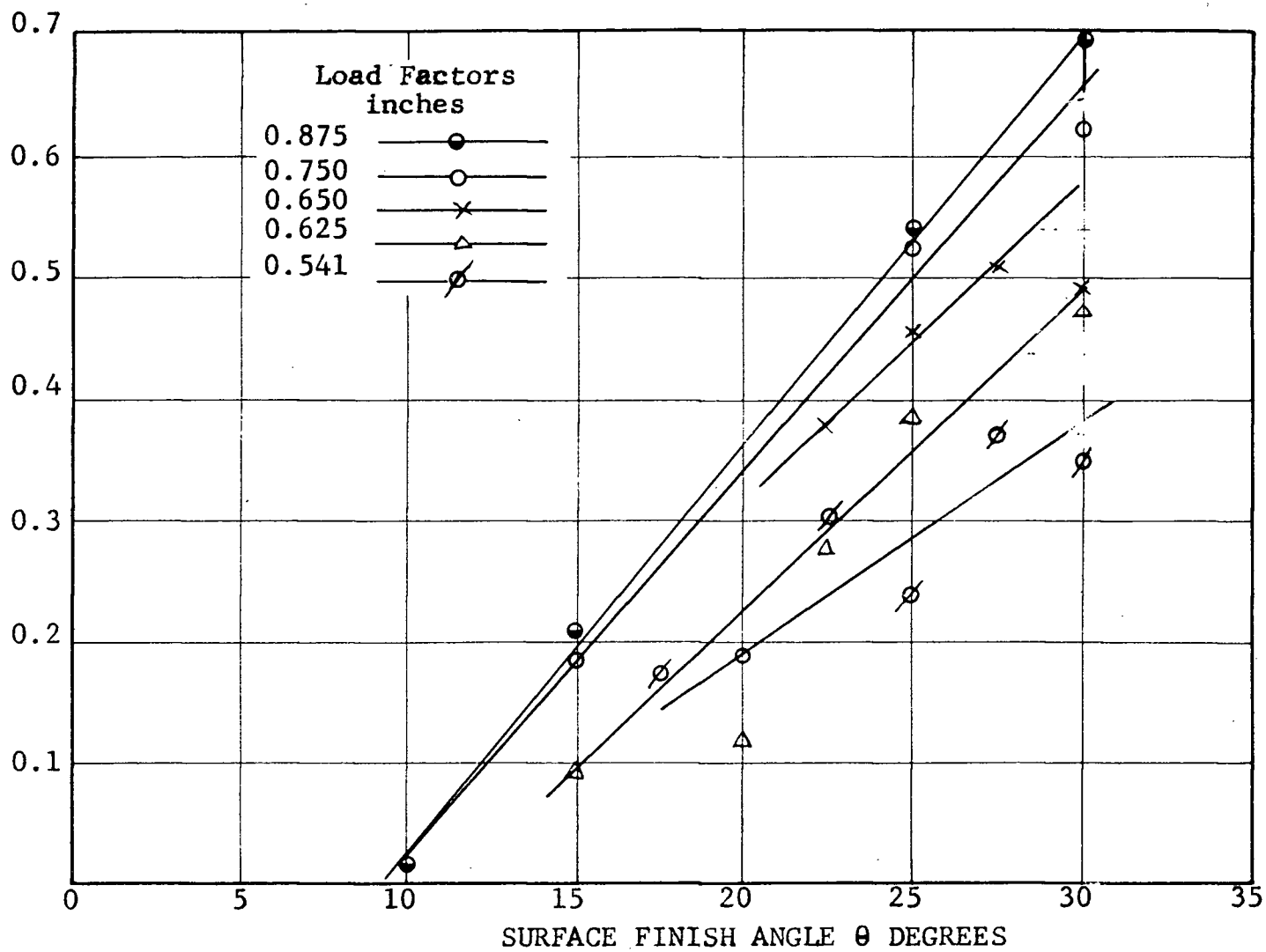

FIGURE 13

VARIATION OF SIMULATED WEAR WITH
SURFACE FINISH FOR VARIOUS LOAD FACTORS

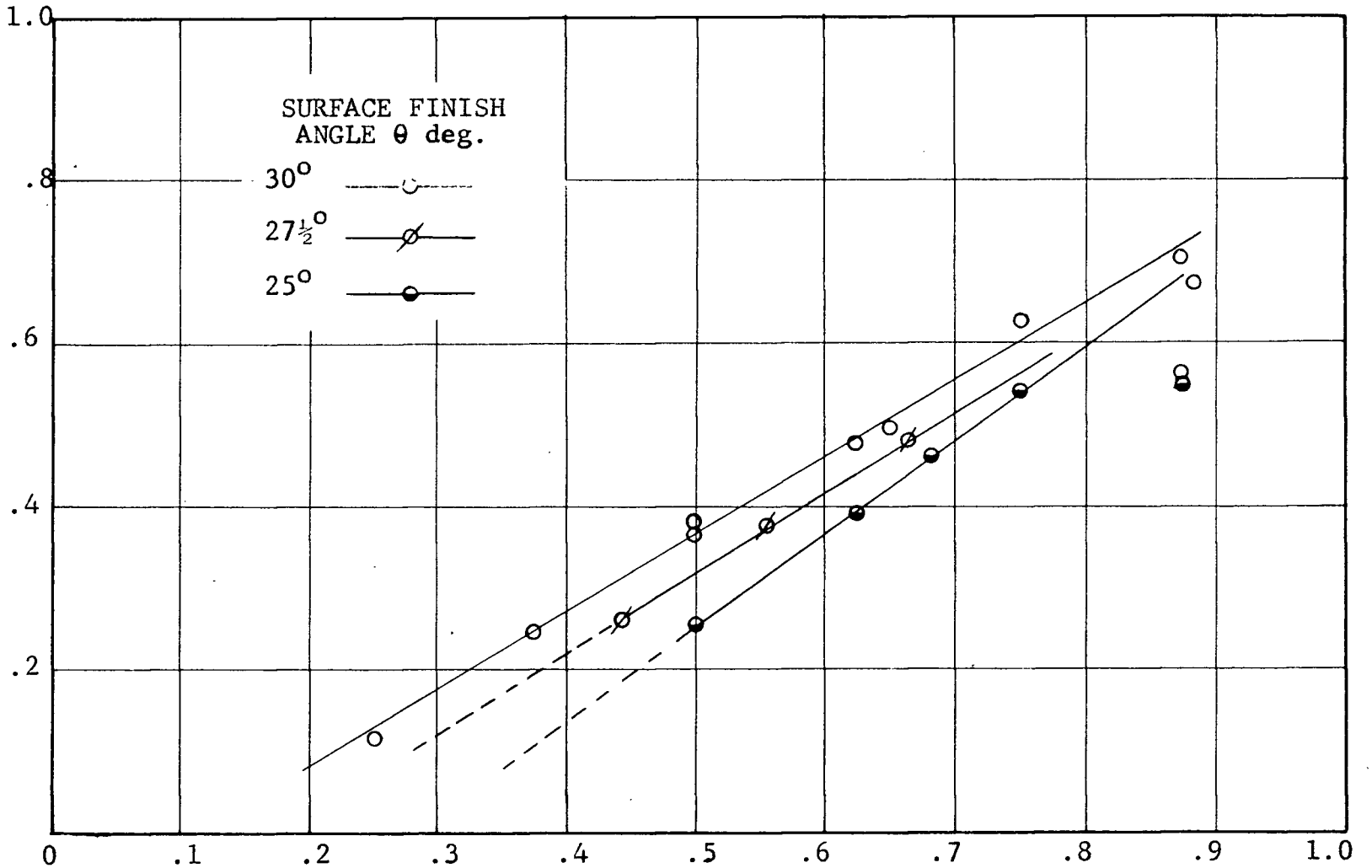

FIGURE 14

VARIATION OF SIMULATED WEAR WITH LOAD FACTOR FOR VARIOUS VALUES OF SURFACE FINISH ANGLE

D. Wear versus Load Factor

The curve for simulated wear versus load factor for three surface finish angles is presented in Figure 14. This is a cross-plot of Figure 13 and all the variables have been previously described. There is very little scatter on these curves except at the highest load factor. The curves have the following positive slopes, showing a decrease in wear for decreasing load factors;

$\theta = 30^{o}$ Slope = 0.94

$\theta = 27\frac{1}{2}^{o}$ Slope = 0.805

$\theta = 25^{o}$ Slope - 1.16

E. Wear versus Simulated Asperity Height

The variation of simulated wear with asperity height is shown graphically by Figure 15. Asperity height is defined as the distance between the tip of an asperity and the main surface as shown in the upper left corner of Figure 15. Using the model junctions this height was varied from 0.6875" to an interlocked position whereby asperities have their tips in contact with the other surface. The particular angle chosen was 30 deg. with a load factor of L = 0.625. inches since the particles resulting from these junctions gave reasonably good results for the variation of wear versus surface finish angle, (See Figure 13). The scatter of points on this particular curve is plus or minus 5%. The curve shows a decrease in wear with decreasing asperity height, the positive slope being approximately 0.14.

II. FRICTION

A. Calculation

The friction results require some explanation

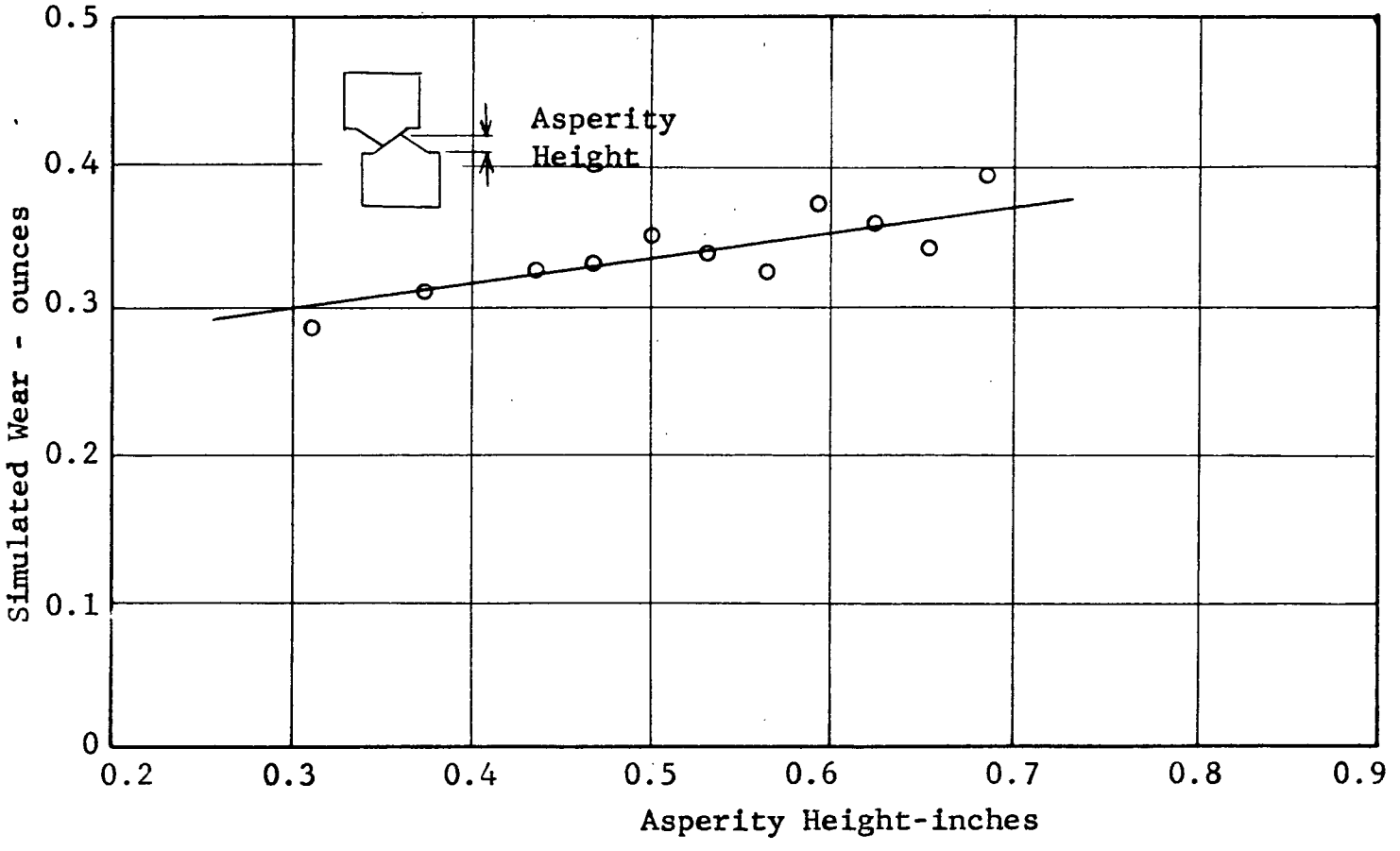

FIGURE 15

VARIATION OF SIMULATED WEAR
WITH ASPERITY HEIGHT FOR L = 0.025 inches
AND θ = 30 degrees

regarding the determination of the simulated coefficient of friction from the force measurements. Since the coefficient of friction is defined as the ratio of the friction force to the normal load, the simulated coefficient of friction could best be determined by the ratio of the areas under the oscillograph curves obtained during the deformation of a model junction. The curves for two such junctions are presented in Figures 16 and 17. The first figure contains the curves resulting from the deformation of a junction with $\theta = 15^{o}$ and L = 5/8". From the ratio of the areas the coefficient of friction was found to be 3. The second set of curves is for a 30 deg. junction with L - 7/8". These curves are similar to Figure 16 up to a displacement of 1.2". Beyond this displacement the latter set of curves are irregular. These irregularities can be explained by an examination of the deformation process previously described. (Figure 11). The normal force results from the parallel sliding of the asperity pair. This will be a compressive force and is assumed positive in this discussion. When a particle is formed, such as was the case here, the junction fails in double shear. The shearing action, as was pointed out in the first part of this chapter, did not progress simultaneously on both asperities. Therefore as one asperity failed, a tensile force resulted between the asperities. This caused the normal force to drop below zero at a displacement of 1.4 inches in Figure 17. Subsequently the shearing of this

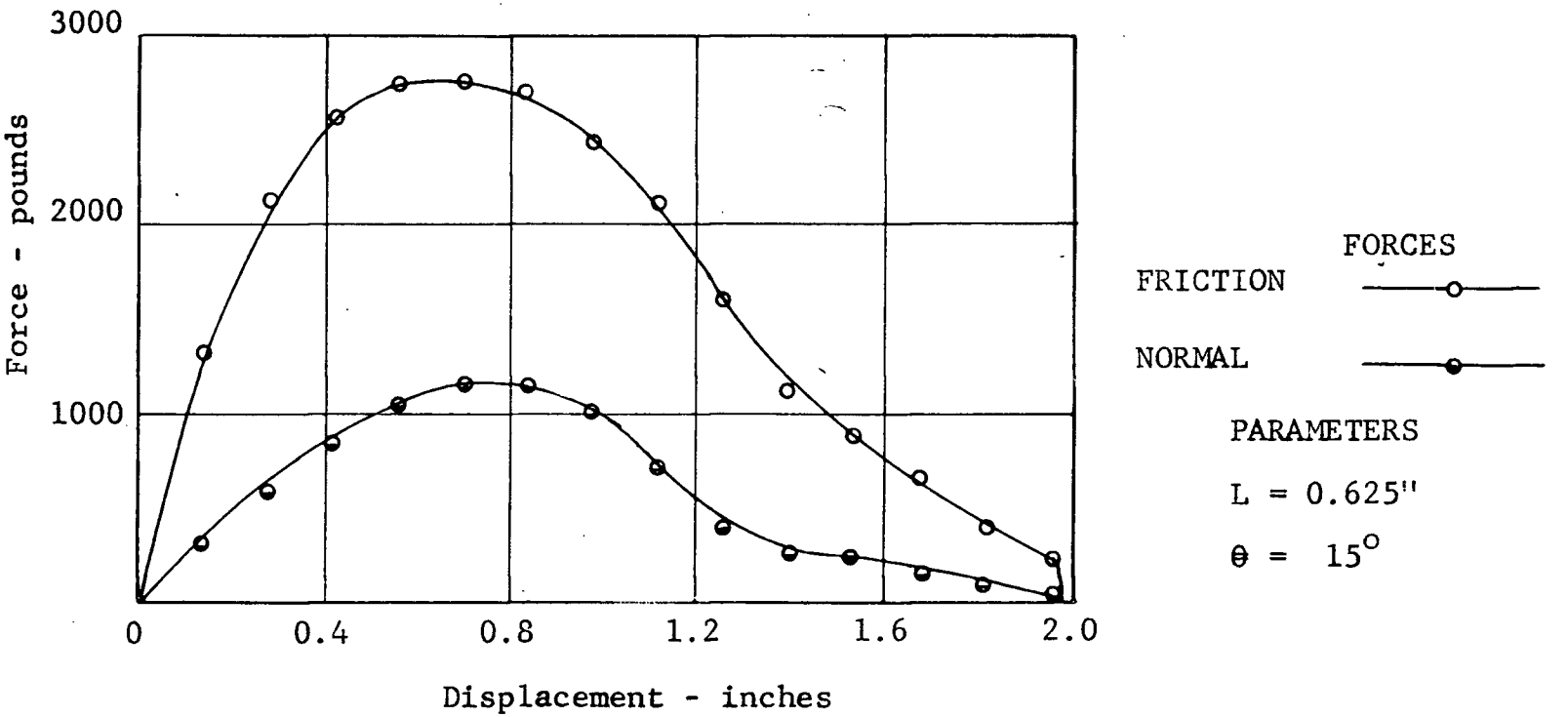

FIGURE 16

FORCES OVER THE LIFE CYCLE
OF A JUNCTION WITH A SMALL SURFACE
FINISH ANGLE. SINGLE
SHEAR FAILURE

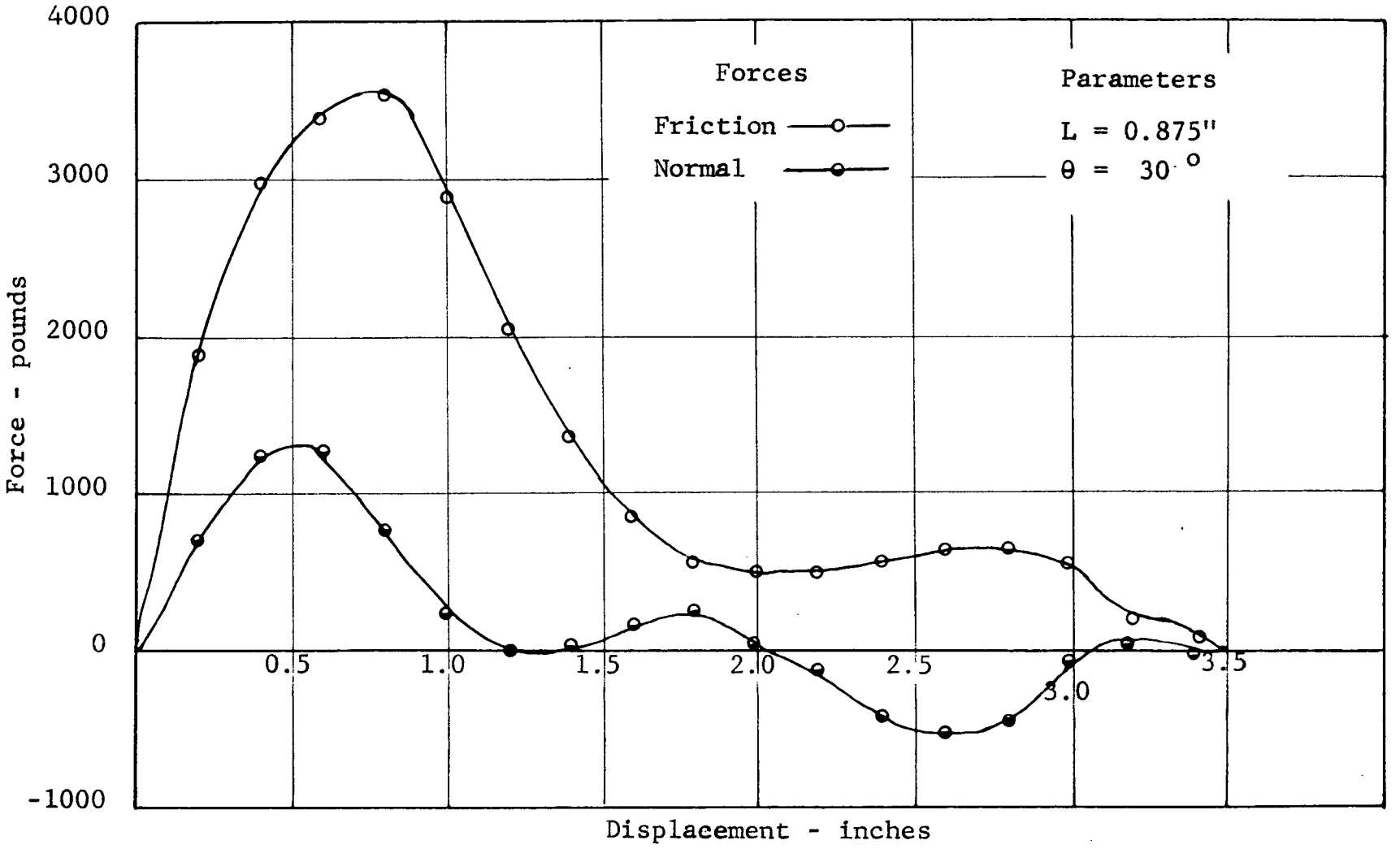

FIGURE 17

FORCES OVER THE LIFE CYCLE OF A MODEL
JUNCTION WITH A LARGE SURFACE FINISH ANGLE
DOUBLE SHEAR FAILURE

asperity slows down and the other starts. At this time the particle is rolled between the two asperities causing a greater compressive force, with the result that the normal force becomes positive again. As failure of the first asperity ceases completely and the other proceeds, the normal force again becomes negative at 2.05 inches. At this stage the normal force is more negative than it was earlier since the compressive action is greatly reduced by the out of plane bending. Meanwhile the friction force has reached a minimum at a displacement of 2.0 inches and then increased slightly before fracture. This behaviour can be attributed to the particle bending out of plane and causing additional shear stress. The type of failure described above made it difficult to assess the curves after the normal force became negative. Another difficulty was in the determination of the true point of fracture of the junction, since with a small angled junction of large load factor the metal was severely cramped between the jaws of the apparatus. This action also contributed to distorted force measurements. These difficulties were overcome by calculating the coefficient of friction at the symmetrical position, Figure 11b. This procedure not only solved the above mentioned problems but it also overcame the problem whereby beyond the symmetrical position the out of plane bending could have influenced the friction values.

The coefficient of friction obtained in this fashion was designated fs and is used in the presentation of the following results.

B. fs versus Surface Finish Angle θ.

The variation of the simulated coefficient of friction with surface finish angle is shown graphically in Figure 18 for various load factors. For the higher values of L (L>½") the curves are generally horizontal, but rise sharply between 20 and 25 degrees. The two curves for L = ¼" and 3/8" have a negative slope to about the 25 degree surface finish angle and then rise at 30 degrees. The curves are plotted separately in Figures 19 (a) and (b), due to the crowding on the combined set of curves.

C. fs versus Load Factor.

A cross-plot of the above results is presented in Figure 20, where the variation of fs with load factor is shown for various surface finish angles. With the exception of the 25° junction these curves all have a negative slope of approximately 2.5, for L = 0.375 inches. The 25 deg. curve has a slope of 0.24. For L = 0.375 there is a sharp rise in fs with the exception of the 25° case, which remains comparatively flat.

D. Deformation of Thick Model Junctions

The two thick junctions investigated had a surface finish angle θ = 25° and a load factor L = ½ inch. Sequence photographs of the failure of one of these junctions is presented in Figure 21. The initial mode of failure was similar to that shown in Figure 11, but there was no simulated particle formed and there was no evidence of out of plane bending. The simulated coefficient of friction at the

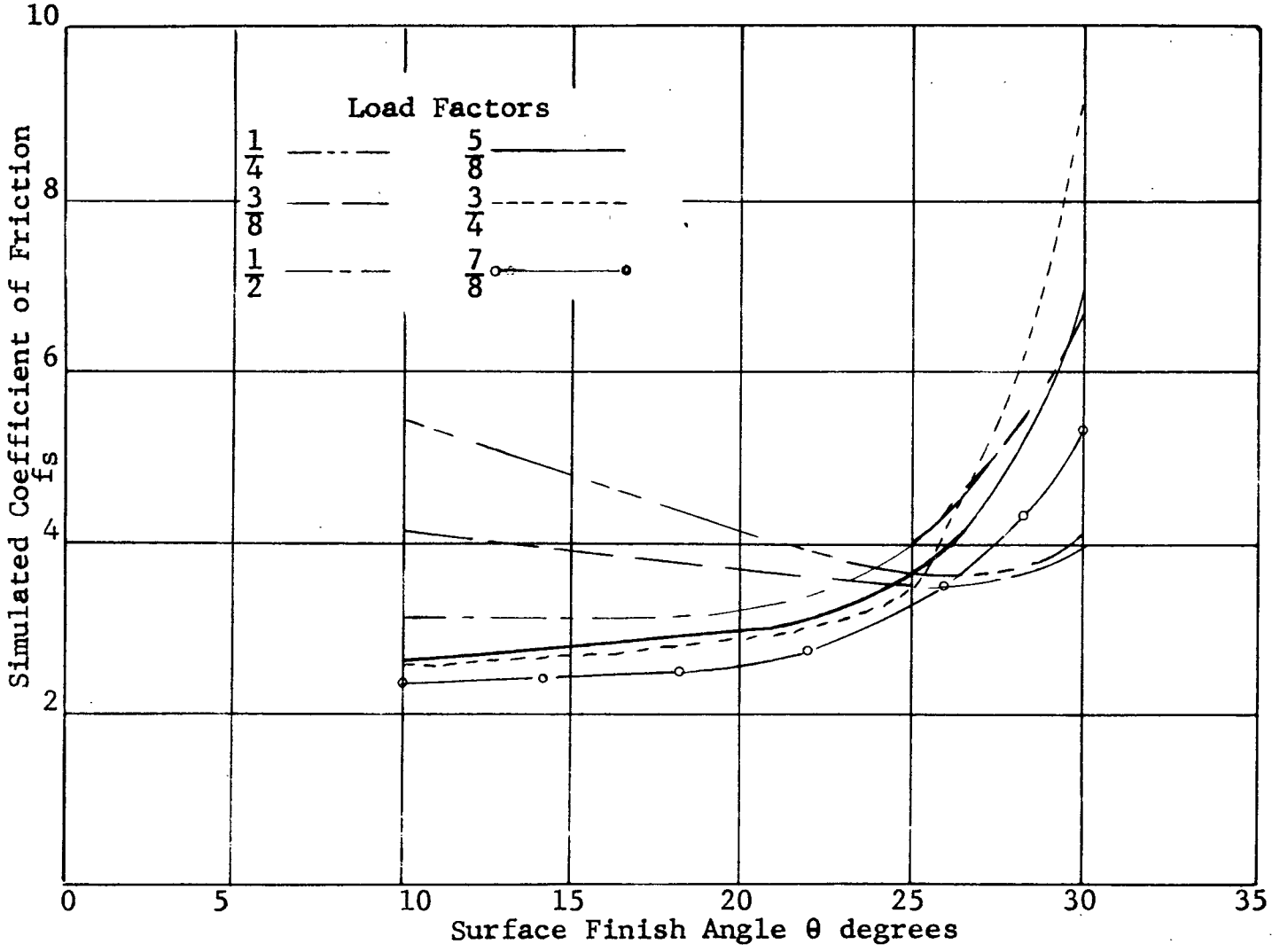

FIGURE 18

VARIATION OF SIMULATED COEFFICIENT OF FRICTION WITH SURFACE FINISH FOR VARIOUS LOAD FACTORS

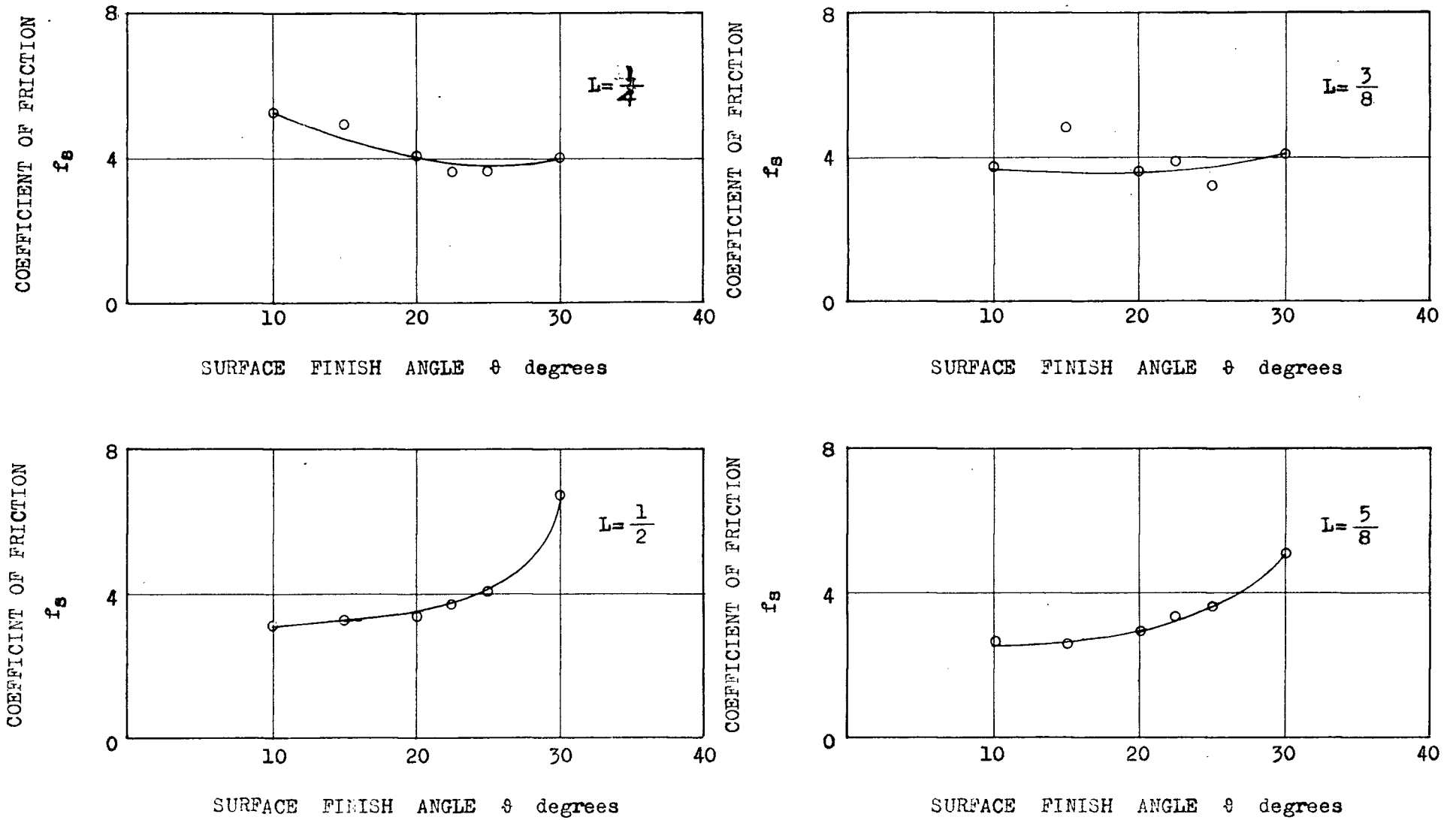

FIGURE 19a

VARIATION OF COEFFICIENT OF FRICTION WITH SURFACE FINISH
FOR SIMULATED METALLIC JUNCTIONS

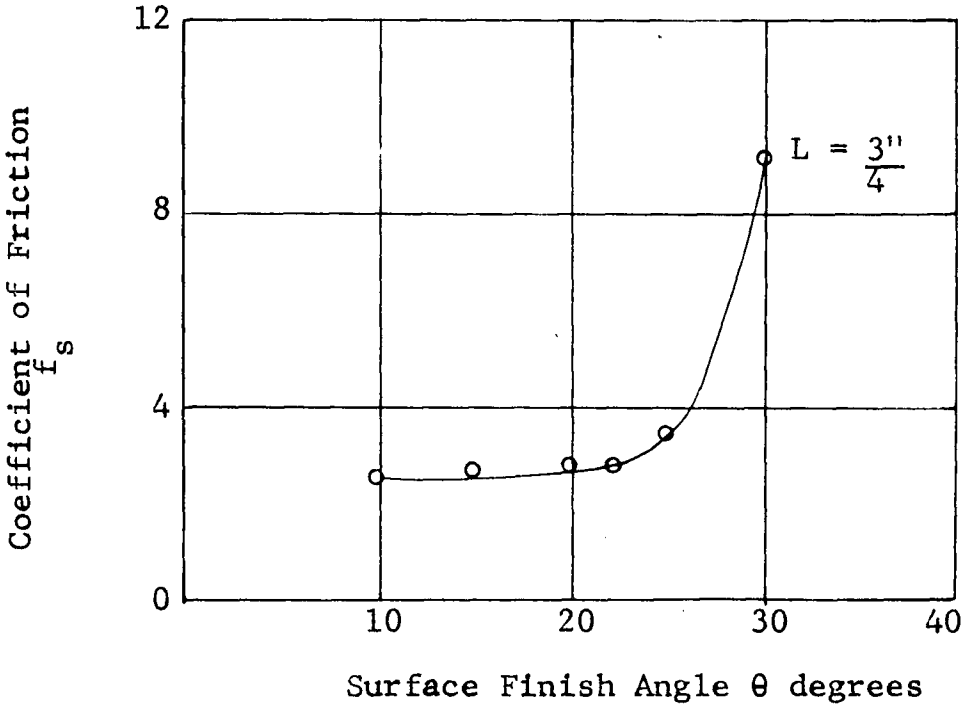

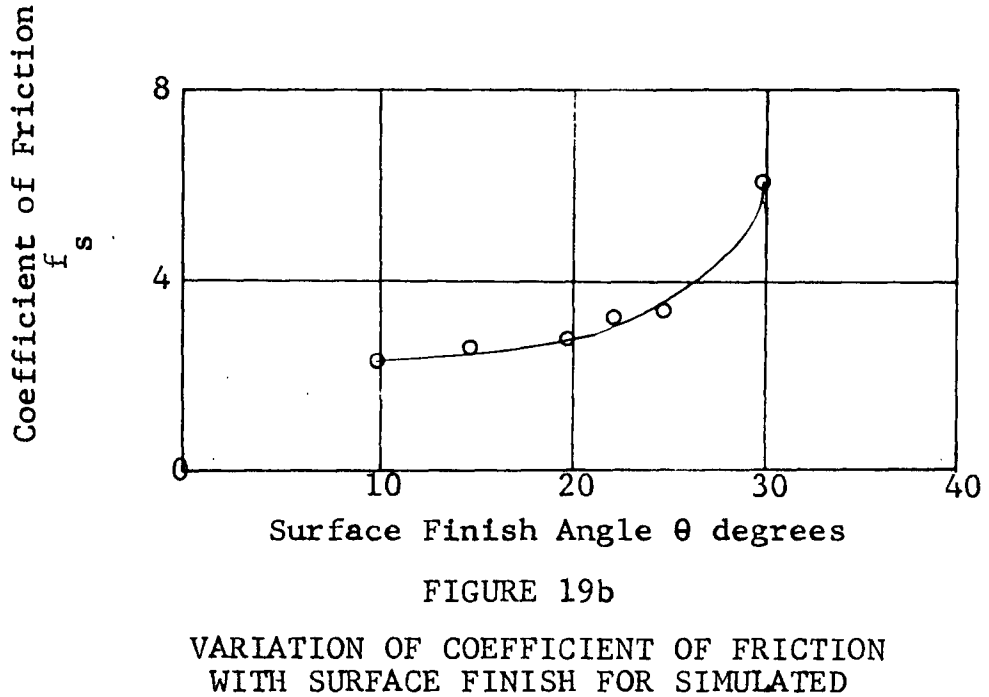

FIGURE 19b

VARIATION OF COEFFICIENT OF FRICTION WITH SURFACE FINISH FOR SIMULATED METALLIC JUNCTIONS (continued)

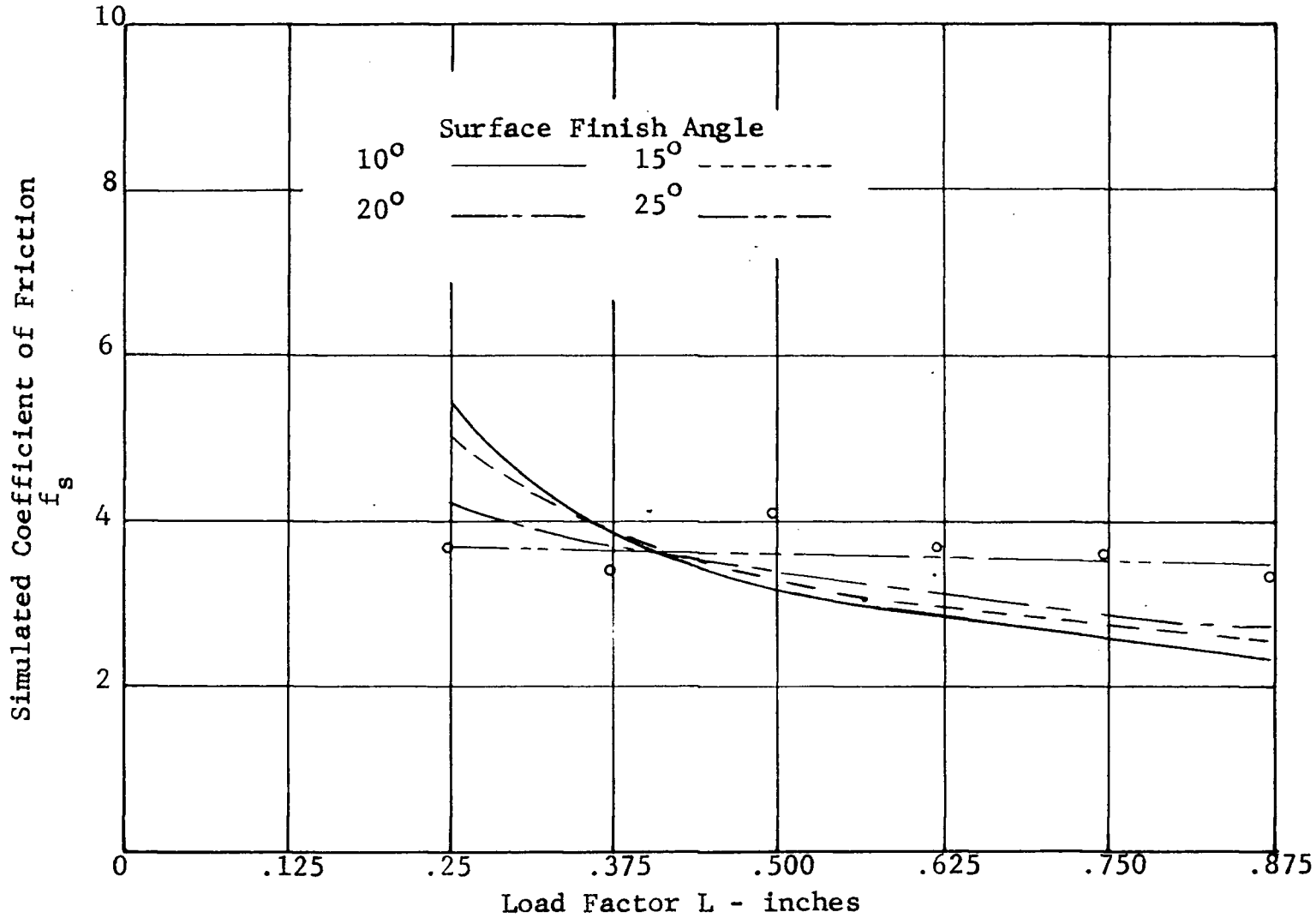

FIGURE 20

VARIATION OF SIMULATED COEFFICIENT OF FRICTION
WITH LOAD FACTOR FOR VARIOUS SURFACE FINISH ANGLES

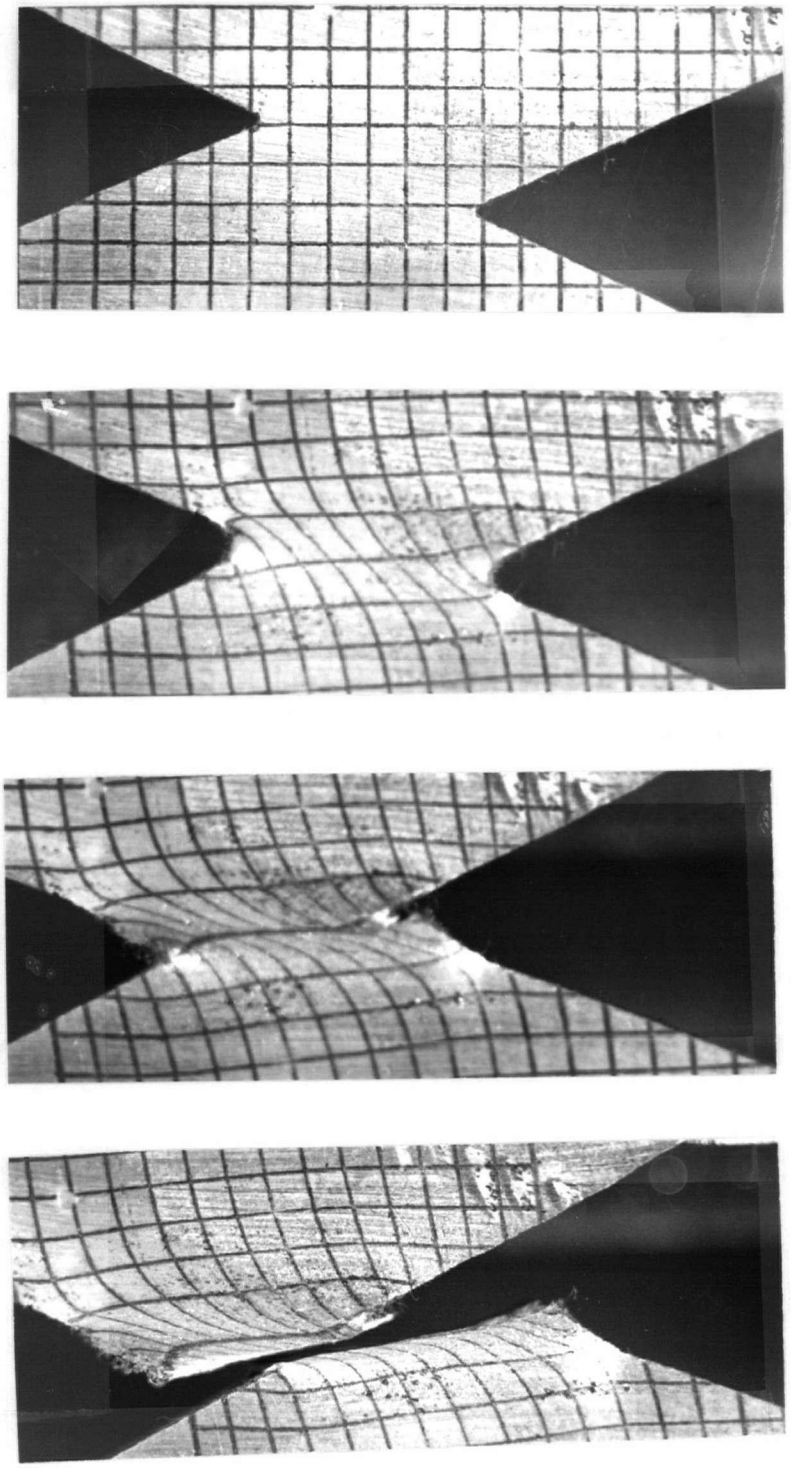

FIGURE 21

DEFORMATION OF A THICK
JUNCTION $\theta = 25^{\circ}$ L = 0.625"

symmetrical position for these junctions was approximately 8.5.

E. Variation of Wear and Friction with Velocity.

Figure 22 shows the results of the investigation of the influence of velocity on friction and wear. The relationship between both these variables and velocity is nearly a horizontal line. There is a slight amount of scatter but no more than was found in the previous results.

The results will be discussed in detail in the next chapter and they will be correlated with experimental evidence obtained using actual surfaces.

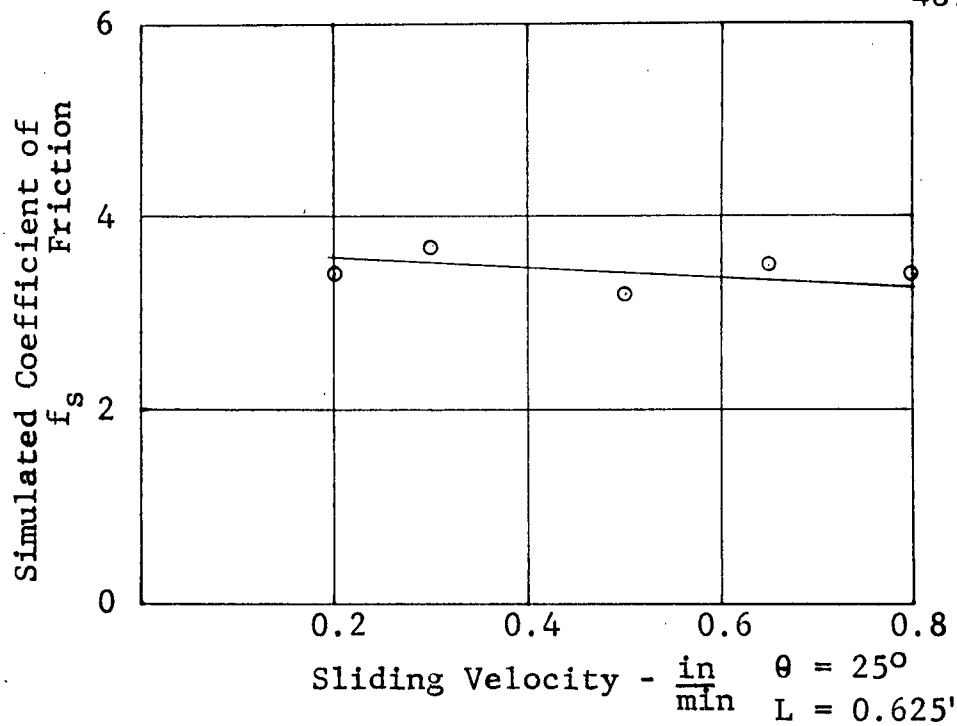

(a) VARIATION OF SIMULATED COEFFICIENT OF FRICTION WITH VELOCITY

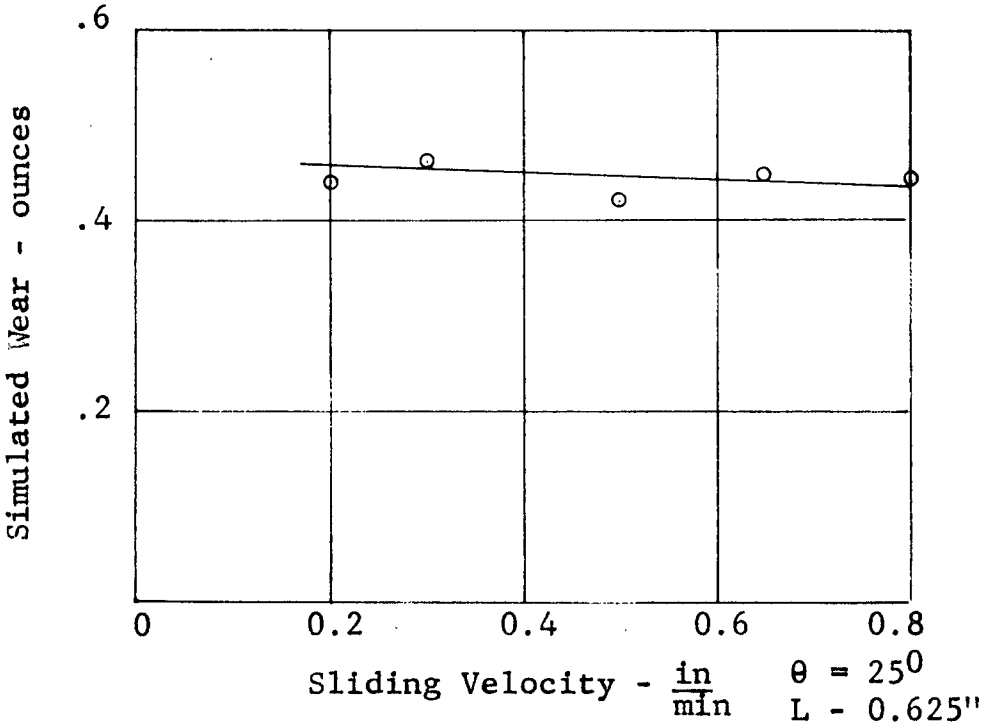

(b) VARIATION OF SIMULATED WEAR WITH VELOCITY

FIGURE 22

INFLUENCE OF VELOCITY ON FRICTION AND WEAR

CHAPTER V

DISCUSSION OF RESULTS

Copper was used exclusively in this investigation but this by no means restricts the interpretation of the results to copper surfaces. The formation and fracture of actual junctions should be the same for a wide range of metals. If the sliding surfaces are of two different metals, the metal transfer will make them similar, as discussed previously. Metallic junctions can be formed and they could fracture in a manner similar to the model. Metals other than copper will have different values for yield pressure and shear stress. The difference in properties will influence the value of the coefficient of friction and wear magnitude, but the mechanism itself should remain essentially the same. With this important feature in mind, the various correlations can be made and the results discussed.

I. WEAR

A. Correlations

Simulated wear can be correlated with actual wear both qualitatively and quantitatively. Firstly, the shape of the particles resulting from the failure of the model junction is similar to the "lens" shape of the actual wear debris studied by Brockley[11] with an electron microscope. The latter particles have a ratio of diameters of approximately 10 whereas the simulated

particles may have a ratio approaching 1 for large surface finish angles. Secondly, a qualitative comparison between simulated wear and actual wear can be made on the basis of wear versus load. Figure 23 gives the wear load relationships for two metals sliding on tool steel[17]. The wear is given

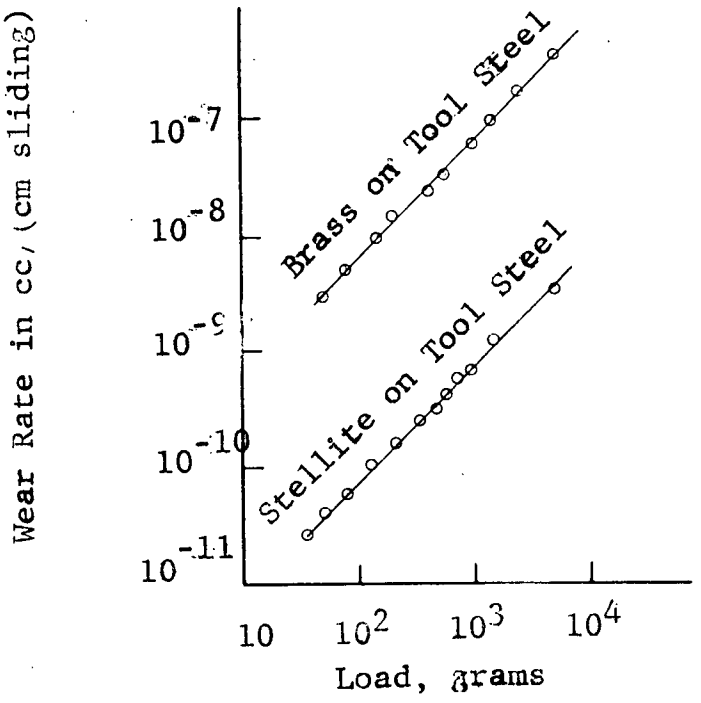

Figure 23
Normal Wear-Load Relationships

as a weight loss divided by the distance travelled. This is to be compared to the wear of the simulated junctions which is given as a weight. Dividing the particle weight by the distance travelled has the effect of lowering the slope of the curves since wear is directly proportional to the distance travelled[17]. This effect is demonstrated

in Figure 24 for the simulated junctions with $\theta = 30^{o}$, and where the distance travelled is the total deformation of the junction over its life cycle. Comparing the curves of Figure 23 with those of Figure 14 and 24, the linear relationship between wear and load is evident in both cases. This general trend serves to indicate that the model junction simulation is valid. Additional proof of validity will be brought out in the discussion of friction.

B. Wear versus Surface Finish.

Although the author was unable to find anything in the literature pertaining to the relationship between wear and surface finish, these relationships can be examined on the basis of the model junction. The variation of wear with surface finish indicates that surfaces with small asperity angles give the least wear. The height of the asperities did not influence the wear very greatly (Figure 15), although there is a slight decrease in wear with decreasing asperity height. These two points indicate that if the model junction simulation is valid, the best surface with regard to wear is one with small asperity angle with the magnitude of asperity height having little influence.

C. Photoelastic Study

The photo-elastic model illustrates two important points:

1) The stress concentration at the notches,
2) The contours of constant shear stress which are the same shape as the particles.

These two facts give visual proof of the start of particle formation and the shear lines. However, a more

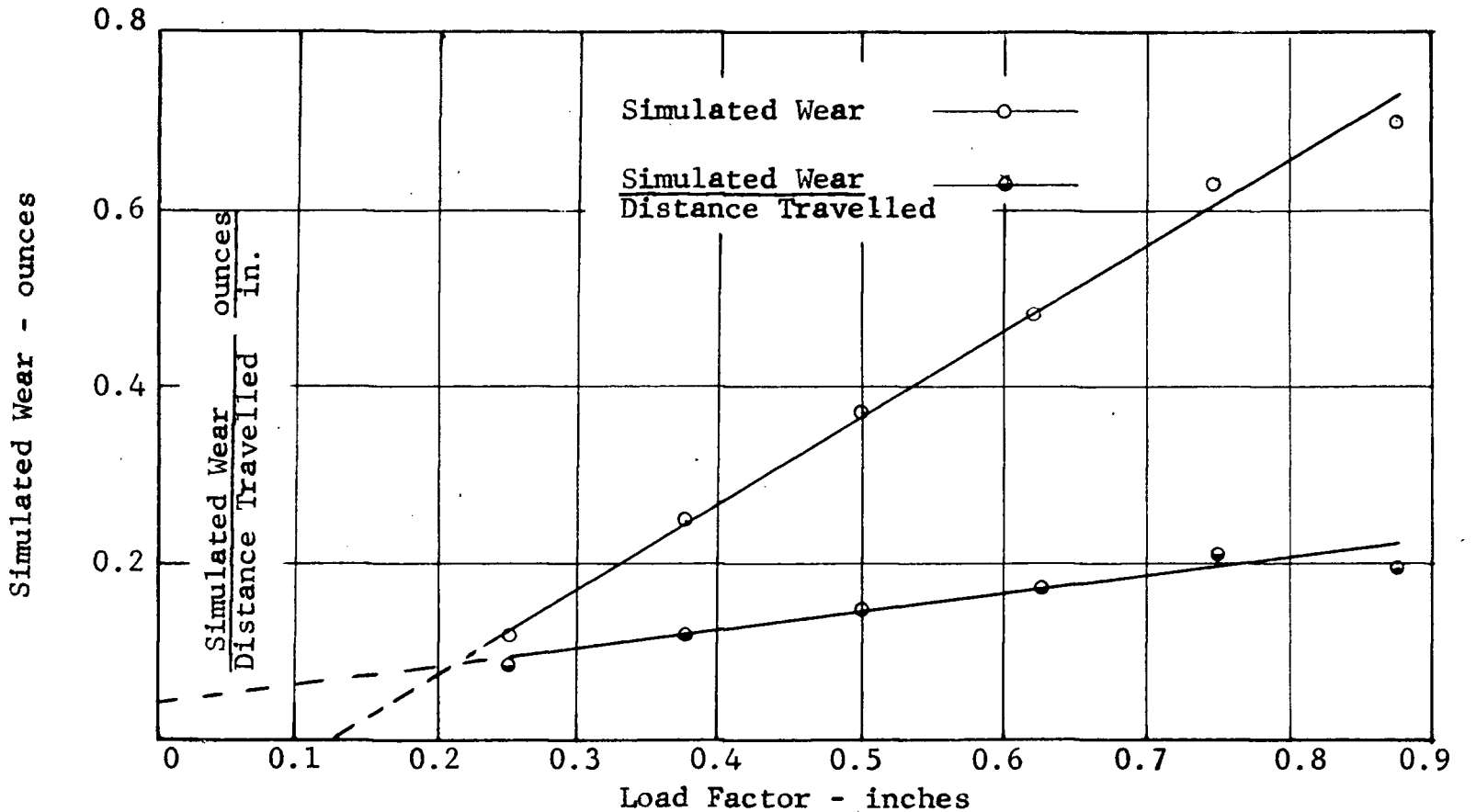

FIGURE 24

WEAR AND SIMULATED WEAR
DIVIDED BY DISTANCE
TRAVELLED WITH LOAD FACTOR

important result of the photo-elastic investigation is that it points out a much more accurate method of determining the exact junction stresses and their orientation. This type of analysis has been used well past the elastic region in other work and would be ideal in the study of friction using the model junction simulation.

D. Wear versus Velocity

The results of the simulated wear versus moving asperity velocity suggest that wear is independent of sliding velocity. This is due mainly to the small velocity range available with the apparatus in its present state. The effect of velocity on wear using the model junction could be investigated further with the existing apparatus with a few small changes in the drive in order to allow for a greater velocity range.

To summarize, the wear relationships derived from simulated metallic junctions show good correlation with actual surfaces both on the basis of particle shape and on the basis of variation of wear with load. Some work should be conducted regarding the variation of wear with surface geometry for actual surfaces, so that correlation could be established in this respect. The photo-elastic and velocity investigations also indicate that further studies along those lines would be helpful in the overall analysis of wear.

II. FRICTION

A. Correlation of Model and Green's Theory

A comparison between the friction results and Green's theoretical solution can be made. Figures 15 and 16 represent the forces involved in the fracture of a junction equivalent to Green's strong junction (Figure 5a). All three figures show W reaching a maximum early in the cycle. Green's theoretical estimate, however, shows W to be considerably greater than F at this point; on the other hand the experimental results show the opposite situation. Green gives two reasons for W being large in his analysis.

1) He assumed absolutely no out of plane movement of the junction, which of course would not be the case for real junctions nor for the models.

2) He assumed a plastic rigid material in which the junctions were free to flow plastically but the metal behind them was rigid. This, of course, is not the case with actual metallic surfaces. Real metals are elastic-plastic such that the metal behind the junctions exhibits small deformations.

Both of these factors tend to reduce the theoretical estimate of W, so that Green's curves probably would approach the experimental curves if it were possible to make the necessary corrections.

Green's theoretical curves show that for a strong junction the friction force remains constant for most of the cycle, whereas in the experimental curves it reaches a maximum and then drops off quite rapidly. The theoretical estimate of F is based on a constant shear stress over the life of the junction. The assumption of constant shear stress is incorrect since it has been shown by Greenwood and Tabor [10] that shearing in the presence of a normal load is not the same as when it is absent. In fact, here the normal force will tend to increase the shearing stress, resulting in the variation in friction shown in Figures 16 and 17. The small junction, Figure 16, is practically the same shape as Greenwood and Tabor's [10] soft copper junction and shows the same average coefficient of friction.

The large load factor junction, Figure 17, demonstrates the influence that the double shear type of failure has on the coefficient of friction. The average f here is approximately 8.5 as opposed to 3 for the single shear type of failure. This high value of f is of the same order of magnitude as the coefficient of friction of outgassed surfaces sliding in vacuo [2], where metal to metal contact is assumed by the absence of contaminent films. It was impossible to compare many junctions on this basis because of the crowding between the blocks at smaller angles, but the symmetrical coefficient of friction shows this high value when double shear occurs, (see Figure 18). Above 20^{o} there is a sharp rise in fs except for the two small load factors. These two curves (L = ¼" and L = 3/8") can be disregarded because they do not

meet the requirement for plane strain that the thickness of 1/8" be much less than the other dimensions. Although the author was unable to locate in the literature a relationship between friction and surface geometry for purposes of correlation, the double shear mode of failure gives an indication of why large values of friction are obtained with outgassed surfaces. This type of investigation on actual surfaces is one which could possibly aid in the study of the mechanism of friction.

B. Correlation of Friction versus Load Factor between the Model and Actual Surfaces.

A comparison of the model and actual surfaces with regard to variation of friction with load is of interest. Figure 25 is for steel sliding on electrolytically polished

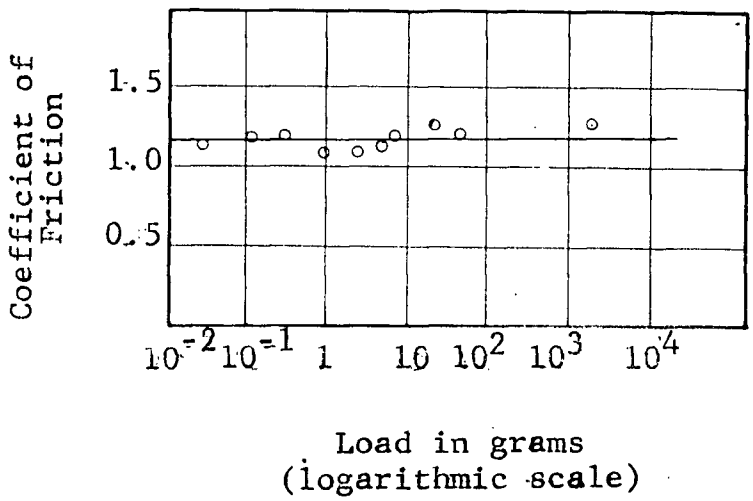

FIGURE 25

VARIATION OF THE COEFFICIENT OF FRICTION WITH LOAD FOR ACTUAL SURFACES

aluminum, and is a horizontal line. This compares quite favourably with the variation of friction with load for the model junction, as shown by Figure 20, except for the

small values of L which can be disregarded because they do not meet the criteria for plane strain as discussed previously. In general the lines in Figure 20 have very little slope and the 25° line is nearly horizontal. Fairly good correlation between the model and actual surfaces is apparent which further substantiates the validity of the model junction.

C. Thick Junctions

The thick junctions showed a large increase in the coefficient of friction as compared to the thinner junctions. This increase in friction can be attributed to the large increase in F with only a slight increase in W. The main reason for the small change in W was that the apparatus was not rigid enough for such a large junction, and relatively large deflections in the directions of the normal force were observed.

No particle was formed in the fracture of the thick junctions. The lack of rigidity probably contributed to this as well as the fact that the load factor was nearly equal to the thickness resulting in a shear break at the narrowest portion of the junction as seen in Figure 21.

The fact that there was no out of plane bending in the fracture of the thick junctions indicates that they might be easier to analyze over the life cycle. Further work in this direction would probably lead to a closer simulation of actual metallic junctions although designing an apparatus that is sufficiently rigid might pose a problem.

D. Friction versus Velocity.

The variation of friction with velocity was investigated. It was found that the simulated friction was

essentially independent of sliding velocity. With actual surfaces, however, friction tends to diminish with increasing velocity.

CHAPTER VI

CONCLUSIONS AND RECOMMENDATIONS

I. Conclusions

The investigation has established the following two wear correlations:

A. The shape of the simulated wear particles is similar to those resulting from the wear of actual surfaces.

B. The wear-load curves for actual surfaces and for the model junction show the same linear relationship.

The simulated friction results indicate that:

A. Green's theoretical estimate of the forces resulting from the deformation of a metallic junction and those obtained in this investigation show general agreement.

B. Friction is independent of load. This result is in agreement with experimental data obtained using actual surfaces.

The model results suggest that:

A. (1) Actual surfaces should have small surface finish angles for minimum wear.

(2) The magnitude of asperity height appears to have little influence on wear.

B. The double shear mode of failure provides an explanation for wear particle formation as well as the large coefficients of friction observed for outgassed metals sliding in vacuo.

The friction and wear results in relation to velocity are inconclusive and require further investigation.

II. Recommendations

A. Future work concerning the relationship between wear and surface finish of actual surfaces would assist in further establishing the validity of the model.

B. The wear and friction versus velocity investigation should be extended by providing the existing apparatus with a greater velocity range.

C. Metals other than copper should be investigated to show that the mode of failure is similar in all cases.

D. Photo-elastic methods, especially photo-elastic coatings appear to provide a means by which the yield pressures and shear stresses could be analyzed more thoroughly.

APPENDIX A.

The following table gives the results of failure tests of six junctions; the simulated friction force determined was used in designing the strain ring.

TABLE 1A**

Junction No.	Hardness Rockwell E or H	Maximum Friction Force lb.
1	63.5 H	2790
2	63.5 H	2450
3	63.5 H	2560
4	63.5 H	2650
5*	82.0 E	3345
6*	82.0E	3200

** These results were obtained on a Tinius Olsen Testing Machine.

* Junctions 5 & 6 were in the "as received" condition as opposed to the others which were annealed at 470° F for 2½ hours and quenched in water.

The stress-strain diagram for junction Number 2 is shown in Figure 1A, along with a sketch of the junction.

From the simulated force determined here, the design loads for the strain ring were obtained. Since junctions twice the thickness of those tested here were to be investigated a value of F = 7000 pounds was chosen. From Greenwood and Tabor's [10] work, the simulated load would then be approximately 2300 pounds, but as a precaution 3500 pounds was used.

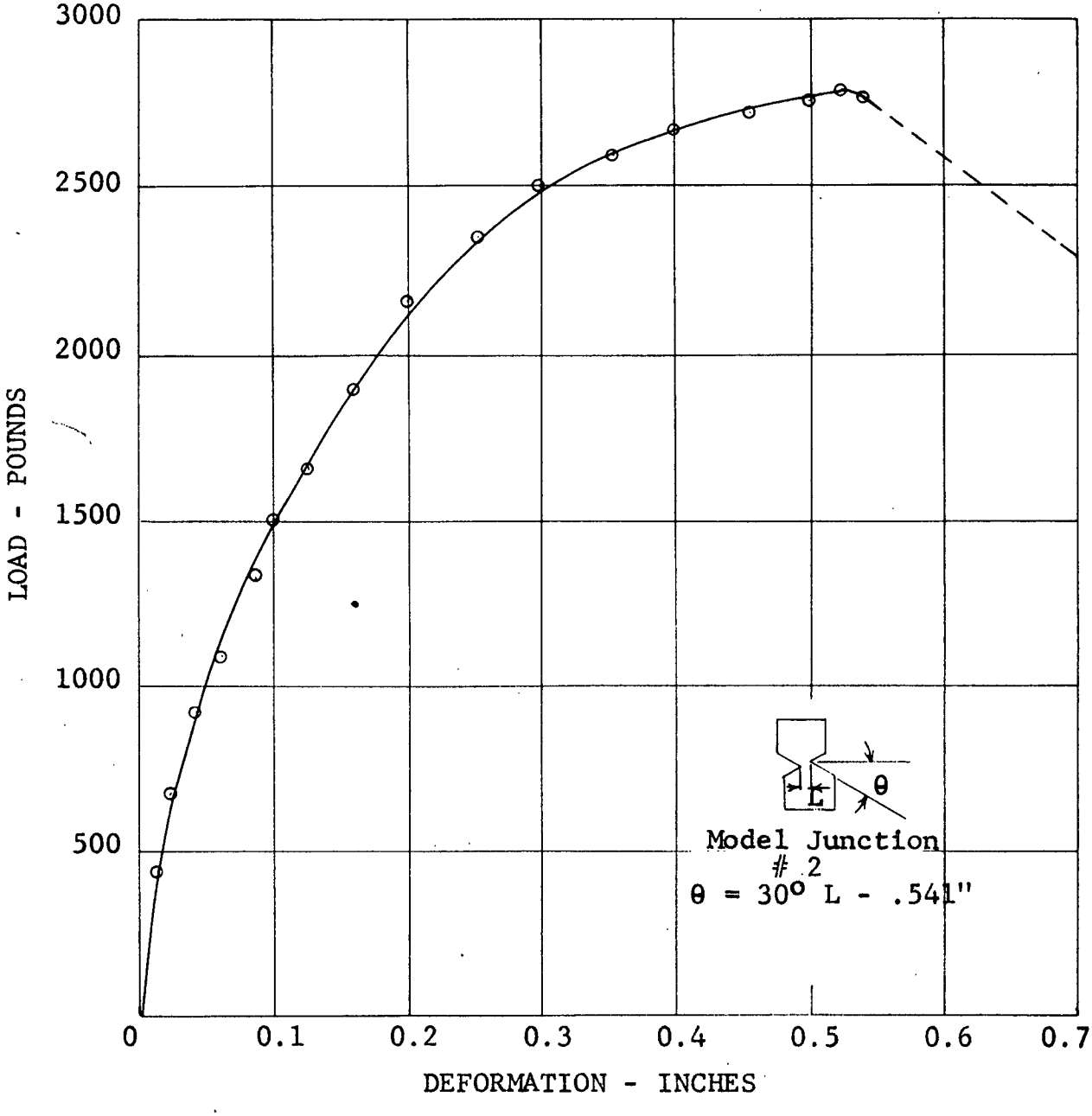

FIGURE 1a

LOAD-DEFORMATION CURVE FOR
A MODEL JUNCTION

APPENDIX B

Strain Ring Design and Calibration

A strain ring is a comparatively rigid device employing electric resistance strain gauges and it is designed to measure a force by resolving it into components. The particular ring used here is shown in Figure 1B and was designed using the approximate equations of Loewen and Cook[16], which are as follows:

$$e_c = 0.7 \frac{VR}{Eb\ t^2} ,$$

$$e_{45} = 1.4 \frac{HR}{Eb\ t^2} ,$$

$$dw = \frac{HR^3}{Eb\ t^3}$$

and $d_f = 3.7 \frac{HR^3}{Eb\ t^3}$ where

R is the mean radius of the ends of the ring, i.e. $\frac{R - r}{2}$, where r is the hole radius, E the modulus of elasticity, b the width and t is the thickness, all in corresponding units; d_w is the vertical deflection due to the force W and d_f the deflection due to F. e_c is the strain at the central gauges and e_{45} is the strain at the gauges on the 45^o faces.

Using the above relationships and the results of shear tests on actual junctions using Brockley's[12] apparatus (see Appendix A) a ring was designed of the following dimensions:

R = 1.366" b = 1.595"

t = 0.700" and L the center to center distance of the holes was 2.3125".

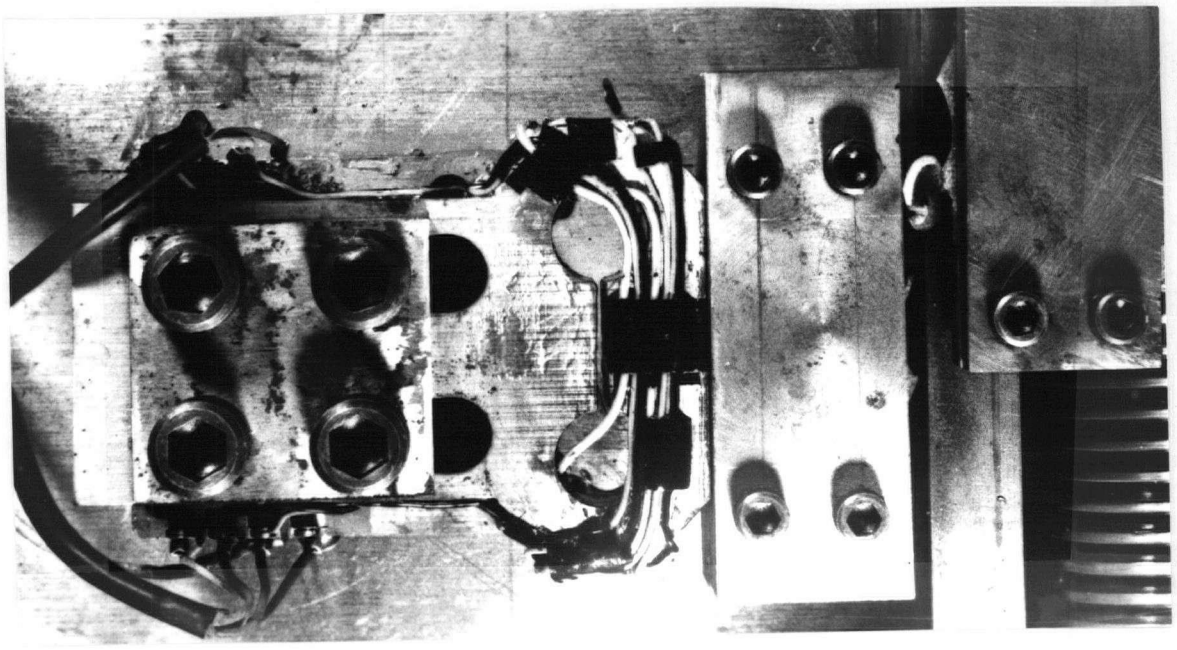

STRAIN RING OPERATING

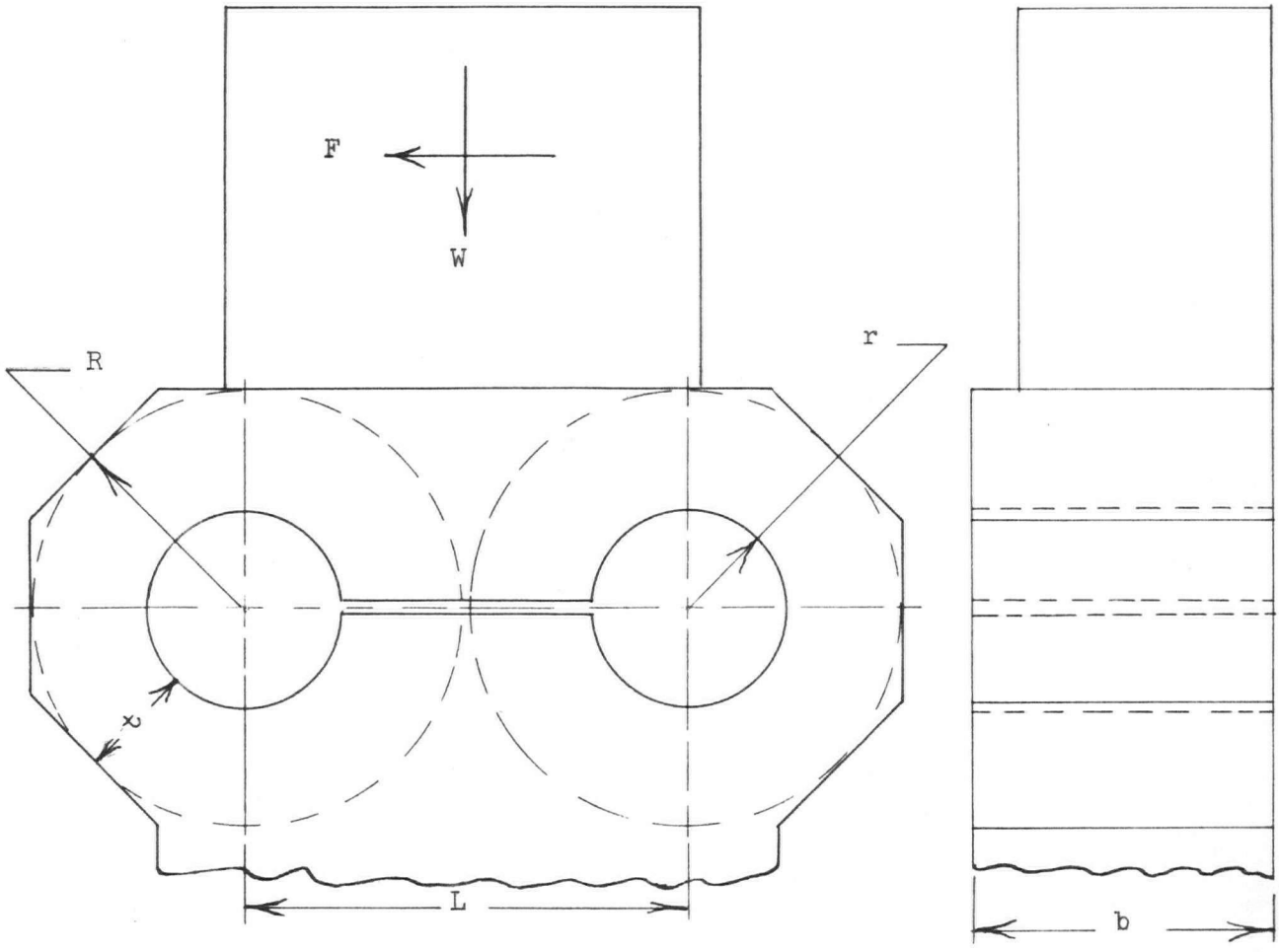

FIGURE 1b

STRAIN RING SHOWING BASIC DIMENSIONS

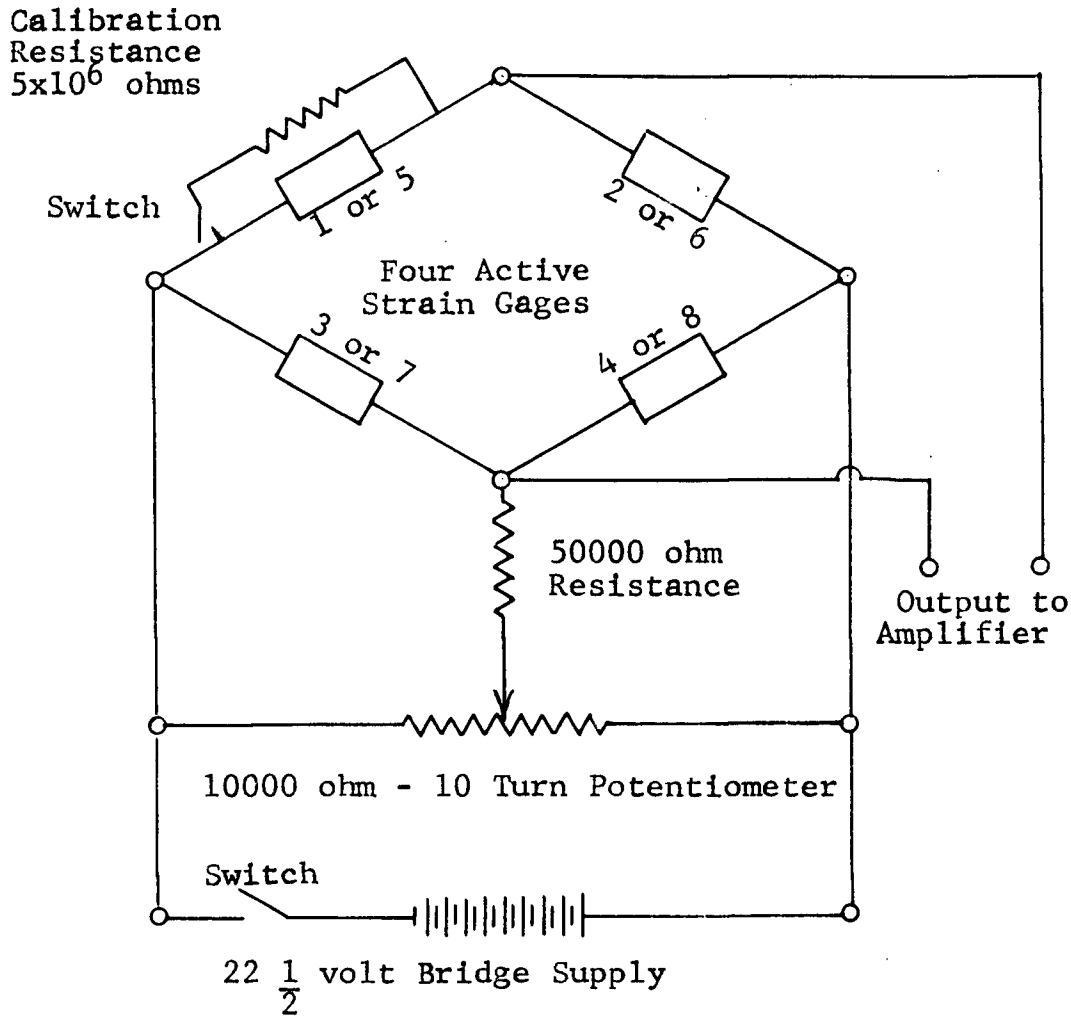

FIGURE 2 b

WHEATSTONE BRIDGE CIRCUIT DIAGRAM

The material selected for the ring was Atlas Steel Company's alloy S.P.S. 245. This is a Chrome Nickel Molybdenum alloy containing 40% Carbon with a trace of Magnesium, Silicon and Phosphorous. The results of three tensile tests of S.P.S. 245 were:

Specimen No.	Yield stress psi	Ultimate stress psi
1	57,800	92,000
2	58,800	91,400
3	56,900	91,700
Average	57,800	91,700

The Wheatstone Bridge circuit diagrams are shown in Figure 2b. The bridge voltages were supplied by 15, 1.5 volt Eveready dry cells. Baldwin-Lima S.R. 4, C-7 isoelastic strain gauges were selected, which had a resistance of 500 ohms and were 1/8" long. A calibration resistance was inserted in each bridge as shown in the diagrams.

CALIBRATION

The strain ring was calibrated in an Olsen testing machine. One force was applied at a time, and the bridge unbalance was recorded on an oscillograph. Any cross effect on the other bridge was also recorded. The calibration curves for various attenuations are given in figure 3B. The ordinate is the calibration load in pounds and the abscissais the oscillograph pen deflection in millimetres. The cross-sensitivities are plotted on the same curves and the slopes of the lines are given.

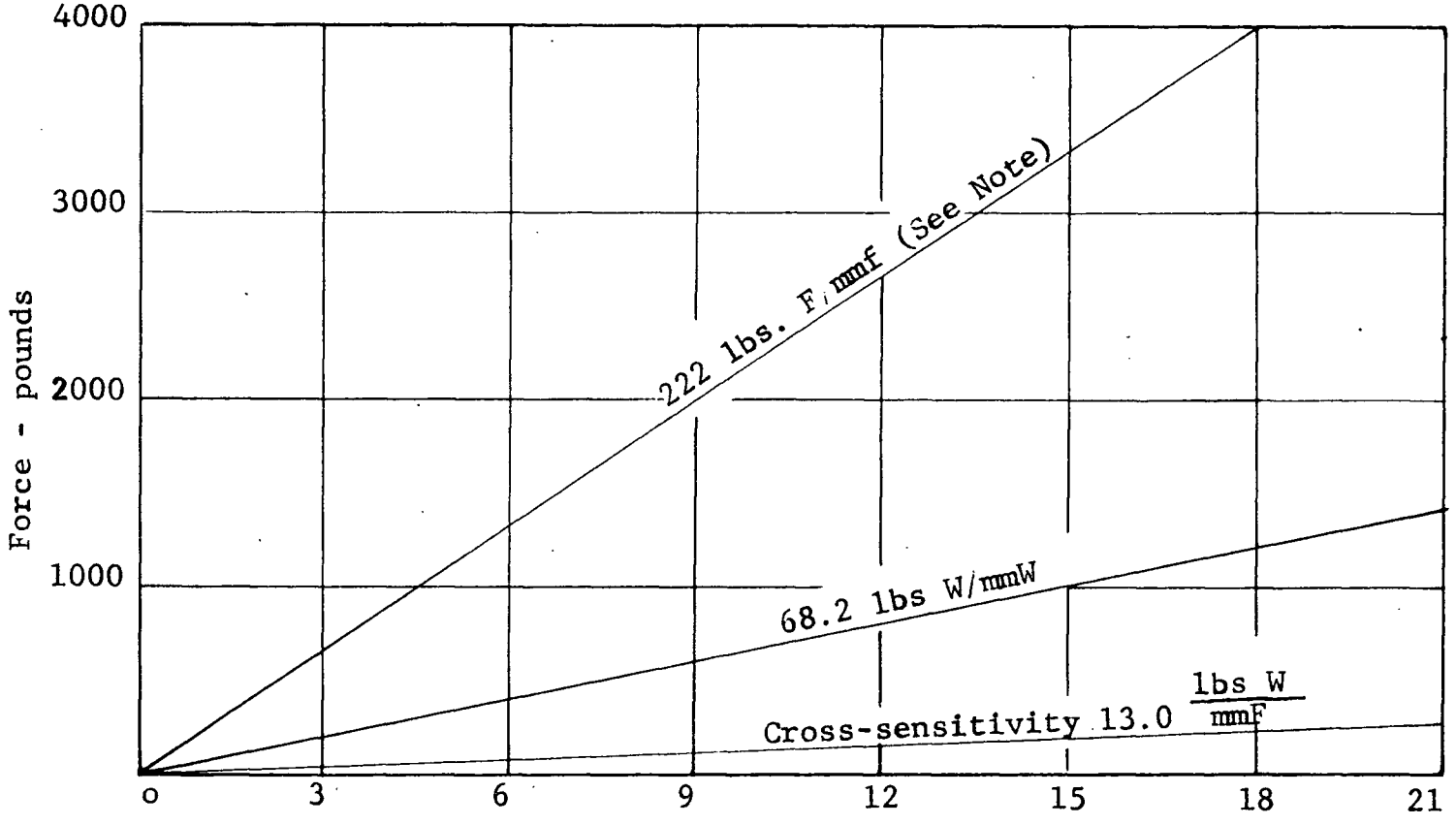

FIGURE 3B(1)

STRAIN RING CALIBRATION CURVE

ATTENUATIONS: FRICTION FORCE X200
NORMAL FORCE X50

NOTE: 222 lbs. friction force per millimeter deflection on oscillograph due to simulated friction force

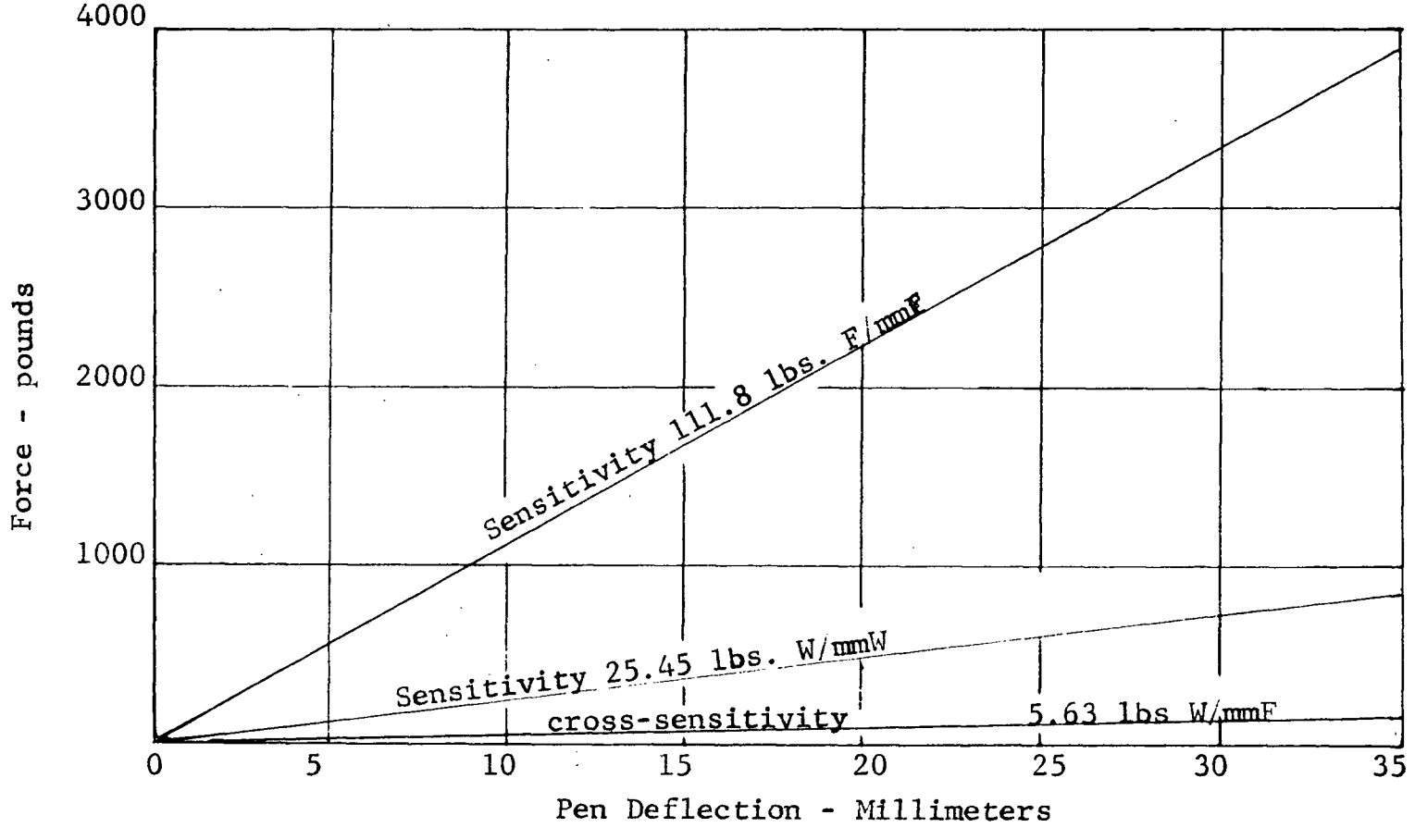

FIGURE 3B(2)

CALIBRATION CURVE

ATTENUATIONS: FRICTION FORCE X100
NORMAL FORCE X20

BIBLIOGRAPHY

1. Green, A.P. "The Plastic Yielding of Metal Junctions Due to Combined Shear and Pressure." Journal of the Mechanics and Physics of Solids. Vol. 2 pp 197 to 211. 1954.

2. Bowden, F.P., and Tabor, D, Friction and Lubrication of Solids Oxford, Clarendon Press, 1950.

3. Shaw, Milton C and Fred Macks. Analysis and Lubrication of Bearings. New York McGraw-Hill Book Company Inc. 1949.

4. Bowden, F.P., Tabor, D. "The Area of Contact Between Moving Surfaces". Royal Societ (London) Proceedings Series A, Vol. 169, pp 391, 1939.

5. Beare, W.G. and F. P. Bowden. "Kinetic Friction". Royal Society of London. Philosophical Transactions. Series A, Vol. 234, pp. 329, 1935.

6. Feng, I-Ming. "Metal Transfer and Wear". Journal of Applied Physics. Vol. 23 No. 9, pp. 1011-19, Sept. 1952.

7. Ernst, H. and M.E. Merchant. "Surface Friction of Clean Metals - A Basic Factor in Metal Cutting Process." Proceedings Special Summer Conference on Friction and Surface Finish. P. 76 Massachusetts Institute of Technology, Cambridge, Mass. 1940.

8. Green, A.P. "Friction Between Unlubricated Metals: A Theoretical Analysis of the Junction Model." Royal Society (London) Proceedings. Series A, Vol. 228, pp. 191-204. 1955.

9. Greenwood, J.A., and D. Tabor. "Deformation Properties of Friction Junctions." Physical Society (London) Proceedings Series B, Vol. 69, Part 9, 609-19, Sept., 1955.

10. Greenwood, J.A. and D. Tabor "The Properties of Model Junctions." Proceedings of the Conference on Lubrication and Wear. The Institution of Mechanical Engineers. pp. 314-17. 1957.

11. Brockley, C.A. "The Wear of Drive Chains". Unpublished Doctor of Philosophy Dissertation, The University of Sheffield. Sheffield, England, 1955.

12. Brockley, C.A. "The Influence of Surface Finish on the Wear of Steel Surfaces." Paper read to the Conference Symposium on Materials Research in Canada. University of British Columbia, Vancouver, B.C. June 6, 7, 8, 1960.

13. Halliday, J.A. "Surface Examination by Reflection Electron Microscopy." Engineer Vol. 199 No. 5178 pp. 569 - 73, April 1955.

14. Thomson, A.S.T., A.W. Scott and W. Ferguson. "Surface Finish of Marine Engine Parts". Institution of Mechanical Engineers and Shipbuilders in Scotland. Paper No. 1131, 1950.

15. The Copper Development Association. Copper Data. London, The Association, 1956.

16. Loewen, E.G. and N.H. Cook. "Metal Cutting Measurements and Their Interpretation" Society for Experimental Stress Analysis. Proceedings. Vol. 13, No. 2, 1956.

17. "Fundamentals of Wear". Lubrication. Vol. 142, pp. 149-160. December 1960.

18. "Nondestructive Testing Handbook" Society for Nondestruction Testing. Ronald Press Co., New York, 1959.